2017

Characterization of Thermoplastics for Leaf Spring Application

Marvin Alejandro Munoz
University of Alabama at Birmingham

CHARACTERIZATION OF THERMOPLASTICS FOR LEAF SPRING APPLICATION

by

MARVIN A. MUNOZ SANCHEZ

SELVUM PILLAY, COMMITTEE CHAIR
ALEJANDRA J. MONSIVAIS
CHARLES A. MONROE
HAIBIN NING

A THESIS

Submitted to the graduate faculty of The University of Alabama at Birmingham,
in partial fulfillment of the requirements for the degree of
Master of Science

BIRMINGHAM, ALABAMA

2017

CHARACTERIZATION OF THERMOPLASTICS FOR LEAF SPRING APPLICATION

MARVIN A. MUNOZ SANCHEZ

MATERIALS SCIENCE AND ENGINEERING

ABSTRACT

Composite materials, especially thermoplastics, are now used extensively in the automotive industry to replace metal components. Three different glass fiber reinforced thermoplastic composites were compared to obtain an equivalent performance of a steel leaf spring. Polyethylene Terephthalate Glycol (PETG), Polyamide 66 (PA6/6) and Polyphenylene Sulfide (PPS) were the matrices considered for this research work. Mechanical testing (tensile, compressive, shear, flexural and moisture absorption) was performed to these three thermoplastic composites concluding that PPS is the best choice since it displayed the best overall properties. Once PPS was selected, a Design of Experiment based on three level (3^k) factorial design, was conducted to define the best processing parameters and their effect on the flexural properties of glass fiber reinforced Polyphenylene Sulfide. Finally, a modification in the architecture of the fiber in the layup was made in ANSYS to define the best arrangement that could withstand not only vertical deflection but also lateral deflection. Two arrangements were simulated and five different fiber angle orientations (0°, 15°/-15°, 30°/-30°, 45°/-45° and 90°) were modeled.

Keywords: thermoplastic, fiber, PPS, PETG, PA6/6, spring

ACKNOWLEDGEMENTS

I would sincerely like to thank Dr. Selvum Pillay for his continuous support and guidance during the course of this research. I would also like to thank my committee members, Dr. Charles Monroe and Dr. Haibin Ning.

I would like to thank the entire Materials Processing and Applications Development staff, MSE composites group, especially to Dr. Mohamed Selim whose advice and support was a great help for me to be able to finish this research successfully.

I would like to thank Rassini Suspensiones, Dr. Alejandra Monsivais and Juan Jose Wong, who I was closely working with to make this research successful, for their continuous support and trust.

Finally I would like to thank my parents who always believed in me and gave me everything to achieve this goal.

TABLE OF CONTENTS

Page

LIST OF TABLES

Tables *Page*

LIST OF FIGURES

Figure *Page*

1. INTRODUCTION

The proposed research is to determine and evaluate alternative thermoplastic composite materials for leaf spring applications without compromising performance. This work is driven by the urgency of finding lightweight materials in the automotive industry to achieve lower fuel consumption in internal combustion engines. The Intergovernmental Panel on Climate Change (IPCC) reports that CO_2 emissions from fossil fuel combustion and industrial processes contributed about 78% to the total Greenhouse Gas (GHG) emission increase between 1970 and 2010 (IPCC, 2014). According to the Laboratory for Energy and the Environment of the Massachusetts Institute of Technology, city/highway fuel consumption in an average lightweight truck could be decreased by 7.6% if 10% of the weight of the vehicle is reduced (MIT, 2008).

Leaf springs, as a structural component, encounter a variety of loading conditions. Therefore it is crucial to account for all types of loadings in order to establish a flexible connection between the wheel and the vehicle´s body (SAE, 2013). The leaf spring should buffer the vertical vibrations or impacts due to road irregularities by means of variations in the spring deflections. In this process, the leaf spring absorbs and/or releases the potential energy of the fluctuating vertical forces, creating a comfortable ride for the passengers in the vehicle (W. J. Yu, 1988). These springs are usually formed by stacking long leafs of steel, in progressively longer lengths on top of each other, so that the spring´s thickness varies along its length.

Composite materials, especially thermoplastics, are now used extensively in the automotive industry replacing metal components (Grauer, Hangs, Martsman, & Tage, 2012) (Geiger, Henning, & Eyerer, 2006). In order to protect natural resources and reduce energy consumption, weight reduction has been the main focus of automobile manufacturers in recent years. Weight reduction can be achieved primarily by the introduction of enhanced materials, design optimization and better manufacturing processes.

Most work in composite materials for leaf spring application has been conducted with thermoset composites (Sancaktar & Gratton, 1999) (Rajendran & Vijayarangan, 2002) (Mathenulla, Sreenivasa, & Jaithirtha, 2014) (Shokrieh & Rezaei, 2003) (Al-Quereshi, 2001) (Deshmukh & Jaju, 2011) (Subramanian & Senthilvelan, 2010) (Papacz, Tertel, Frankovsky, & Kurylo, 2014) (Pandey & Patil, 2014). The focus of this work will be thermoplastic materials. These materials present some advantages over thermoset materials. One of them is the ability of being recycled not only as ground filler (Lopez, Martin, Diaz, Rodriguez, & Romero, 2010) (Mahajan, Swami, & Patil, 2015) (Gaikwad, Sonkusare, & Wagh, 2012). Work done by Henshaw et al. has demonstrated the feasibility of using recycled thermoplastic materials by injection and compression molding (Henshaw & Weijian, 1996). Reprocessability, weldability and reparability are some of the important features that thermoplastic materials have as compared with thermosets (Stavrov & Bersee, 2005). Some of the difficulties when processing thermoplastics are high processing temperatures (compared with thermosets), long cooling times, high viscosity (limits processing techniques) and, for high crystallinity thermoplastics, high shrinkage after processing.

This research is divided into three main sections which are material selection and processing procedures, processing optimization and fiber architecture variation by layup modification.

2. MATERIALS AND METHODS

E-Glass Fiber

A variety of engineering fibers can be found as reinforcement for composites. Based on the intended application a thorough selection must be made. Glass fiber is one of the most used fibers for automotive applications based on its low cost and good mechanical properties (Sanjay, Arphita, & Yogesha, 2015) (Knox, 2008). Depending on the specific application, glass fiber can be tailor made such as Type E (electrical), Type C (chemical), and Type T, for thermal insulation. (Auborg, Crall, Hadley, Kaverman, & Miller, 1991). Figure 1 and Table 1 show a comparison between glass, aramid and carbon fiber cost and mechanical properties respectively.

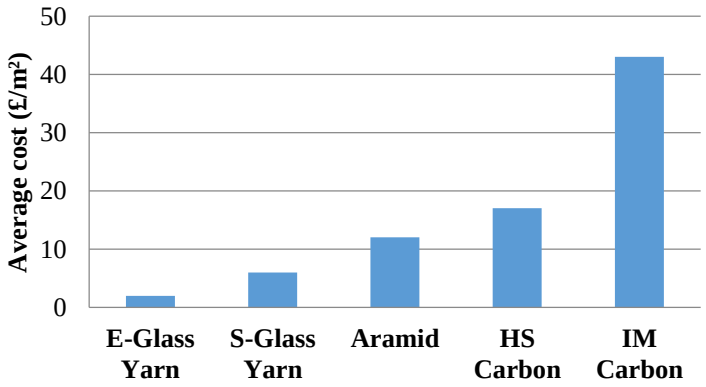

Figure 1.*Average cost comparison between commercially available fibers.* (NetComposites Ltd, 2017).

Table 1.*Comparison between mechanical properties of commercially available fibers.* (NetComposites Ltd, 2017).

Material Type	Tensile Strength (MPa)	Tensile Modulus (GPa)	Density (g/cm^3)	Specific Modulus
Carbon HS	3500	160 - 270	1.8	90 - 150
Carbon HM	3500	325 - 440	1.8	180 - 240
Carbon UHM	2000	440+	2	200+
Aramid LM	3600	60	1.45	40
Aramid HM	3100	120	1.45	80
Aramid UHM	3400	180	1.47	120
Glass - E glass	2400	69	2.5	27

Polyethylene Terephthalate Glycol (PETG)

PETG is semi crystalline polyester (40% crystallinity at most) with a glass transition temperature near 160°F and a melting temperature around 350°F (Gauthier, et al., 1993). The degree of crystallization and direction of the crystallite axis govern all of the resin's physical properties. The percentage of structure existing in crystalline domains is primarily determined through density measurements or by thermal means using a differential scanning calorimeter (DSC). The density of amorphous PETG is 1.333 g/cm^3

while the density of a PETG crystal is 1.455 g/cm^3 (Harper, 2004). It must be mentioned that PETG has the advantage of being processed into prepregs with weight fiber content up to 70% (PolyOne, 2017). This is achieved thanks to the moldability given by the addition of glycol to standard PET. This addition prevents an undesirable crystallization effect that causes standard PET to become brittle.

Polyamide 6/6 (PA 6/6)

PA 6/6 (Nylon 6/6) is one of the most used polymers in engineering applications. This is based on its high elastic modulus, good mechanical strength and dimensional stability at high temperatures (Albano, Sciamanna, Gonzalez, Papa, & Navarro, 2001). One of the main drawbacks in the use of PA6/6 is the susceptibility of polyamides to hydrolytic degradation. Hydrolytic degradation occurs when an amide bond is split into an amine and a carboxylic acid upon reaction with water (Smith, 2016).

When two monomers are used in the fabrication of nylon, two numbers will be used to identify it (PA 6/6). The first number refers to the number of carbon atoms in the diamine used (a) and the second number refers to the number of carbon atoms in the diacid monomer (Harper, 2004).

The amide groups are polar groups and significantly affect the polymer mechanical and thermal properties. The presence of these groups allows for hydrogen bonding between polymer chains, improving the interchain attraction. This gives polyamides good mechanical properties. The polar nature of polyamides also improves the bondability of the materials, while the flexible aliphatic carbon groups give nylons low melt viscosity

for easy processing. This structure also yields polymers that are tough above their Tg (Deaning, 1972).

Polyphenylene Sulfide (PPS)

Polyphenylene Sulfide (PPS) is a semi crystal polymer with a repeating unit in its molecules like shown in Figure 2. PPS is regularly 65% crystalline which is given by the flexibility of its chains as well as the structural consistency of its molecules (Mallik, 2007). It is important to mention that mechanical properties are correlated to mechanical properties; higher degree of crystallinity equals higher mechanical properties. For a leaf spring application, moisture absorption is crucial as the leaf spring will be in contact with a variety of fluids during its lifetime. Some of these liquids include water, motor and transmission oil, brake fluid, etc. According to the work conducted by Soules, D. A. et al, PPS shows outstanding properties against moisture absorption. Thin PPS samples (1.5 mm) were exposed to an environment with 95% relative humidity at 71°C for a period of 14 days. The percentage of moisture absorption was 0.1% which conveniently suits the application in leaf springs (Soules, Hagenson, & Cheng, 1991).

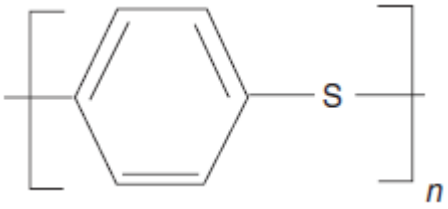

Figure 2.*Repeating unit in PPS molecules.* **(Mallik, 2007)**

Thermoplastic Prepregs

Three different glass fiber reinforced thermoplastic prepregs were considered for this research: Polyethylene Terephthalate Glycol (PETG), Polyamide 6/6 (PA 6/6) and Polyphenylene Sulfide (PPS). The decision of using prepregs was based on processed part uniformity and repeatability, low void content, high specific modulus and strength (along fiber orientation), control of fiber content and its extended shelf life (Thomas, 2013). PA 6/6 and PPS prepregs considered for this research are located in the upper limit of fiber content. PETG on the contrary, its ability to fully wet out fibers allows PETG prepregs to have significantly higher fiber content.

PETG Prepreg

The 6511 PETG prepreg used for this research was manufactured by Polystrand Inc. The industrial e-glass areal weight for this material is 499 g/m^2, tape thickness 0.38 mm and a PE copolymer resin system.

PA 6/6 Prepreg

Celstran CFR-TP PA66 GF60-02 is a 60% E-glass by weight polyamide 66 (nylon 66) continuous fiber reinforced thermoplastic composite tape manufactured by Celanese Corporation. Areal weight for the contained glass fiber is 291 g/m^2, tape thickness and width are 0.3mm and 305 mm respectively.

PPS Prepreg

Celstran CFR-TP PPS GF60-01 PPS is a 60% E-glass by weight carbon black PPS (polyphenylene sulfide) continuous fiber reinforced thermoplastic composite tape produced by Celanese Corporation. The e-glass areal weight for this material is 372 g/m^2, tape thickness and width are 0.25 mm and 305 mm respectively.

Prepreg Fiber Content

Fiber content in composites has a strong impact on mechanical properties. Some specific properties are strongly correlated to fiber content such as tensile and compression properties.

In order to determine the actual fiber content of the unprocessed prepregs, ASTM D3171 (Standard Test Methods for Constituent Content of Composite Materials) was used. In Table 2 a comparison between the theoretical fiber content (provided by supplier) and the experimental fiber content is shown. The matrix burn off testing setup is shown in Figure 3.

$$Fiber\ wt.\% = \frac{W_f}{W_c}$$

Where:

W_f= Weight of the fiber residue after burn off (g).

W_c= Weight of the composite (g).

Table 2.*Fiber weight percentage comparison between the theoretical fiber content and the experimental fiber content of the studied materials.*

	Theoretical Fiber Content (wt. %)	Actual Fiber Content (wt. %)
PETG	65	65.48
PA 6/6	60	60.29
PPS	60	59.63

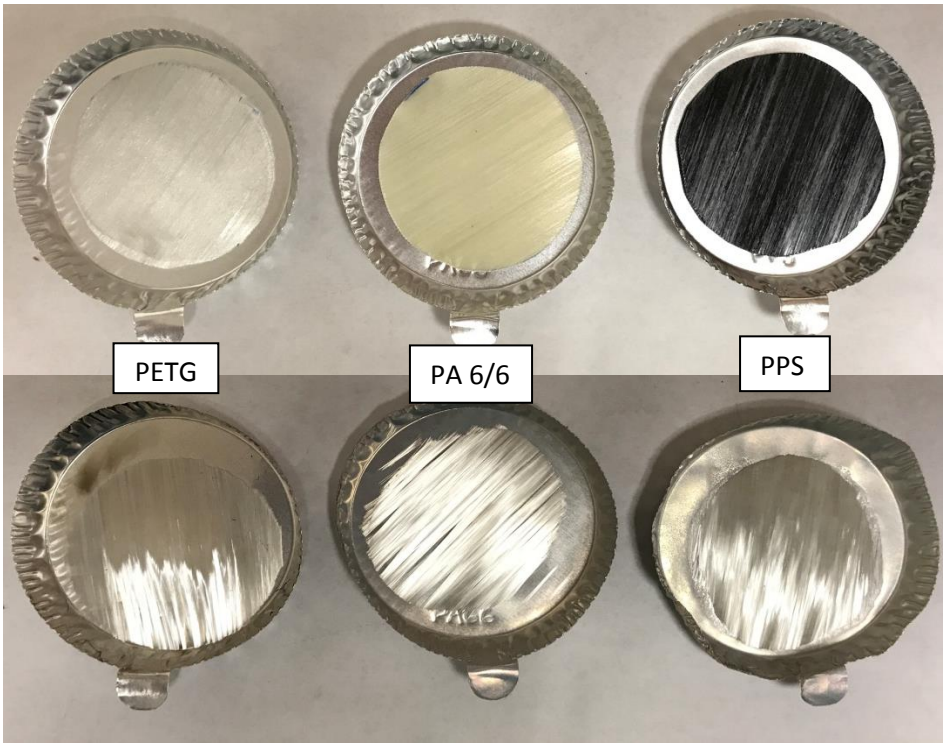

Figure 3.*Matrix burn off samples before (top) and after (bottom) experimentation.*

Sample Preparation

Compression molding is a manufacturing process for composites where sheet molding compounds (SMC), are transformed into finished parts by applying heat and pressure by

a matching tool. This process can be used for both LFT and continuous fiber composites. The compression molding process begins with the placement of precut SMC; usually a stack of several rectangular plies called the preform, onto the bottom half of a preheated mold cavity (Mallik, 2007). Once the preform is sitting in the cavity, pressure is applied by closing both sides of the tool. Heat, normally applied by heated platens, travels through conduction into the preform. It is important to mention that when processing thermoplastics once the preform has reached its melting point, pressure must not change until the sample´s temperature has lowered to its glass transition temperature. The selected processing parameters for each of the studied thermoplastic composite materials are shown in Table 3.

Table 3. *Selected processing parameters for compression molding after conducting DSC analysis on the three analyzed thermoplastic composite materials.*

Material	Processing Pressure (tons)	Processing Temperature (°F)	Tg (°F)	Dwell Time (min)
PETG	10	350	195	10
PA 6/6	10	500	195	10
PPS	10	550	242	10

A four-sided 12” by 12”closed tool was used to process 3 mm thick plates in a 100 ton heated platen press. Each of the heating platens has water lines running across the platen to ensure uniform cooling. Considering the thickness of an individual ply, a stack of unidirectional fiber prepreg was made into the tool before placing on the press. It is important to mention that before ply placement the tool was cleaned with Frekote PCM

mold cleaner. Once the mold was properly cleaned, Frekote 700-NC release interface was applied. Once the plates were processed, samples were cut according to the respective ASTM standard utilizing a water cooled tile saw equipped with a 9”diamond coated blade.

Differential Scanning Calorimetry (DSC)

In order to determine the degree of crystallinity, melting temperature (Tm), glass transition temperature (Tg), Differential Scanning Calorimetry was used. The equipment required to perform this testing was a TA Instruments Q100 paired with a TA Instruments DSC Refrigerated Cooling System. The parameters used for DSC analysis for the three thermoplastic composites materials are shown in Table 3.

Table 4.*Testing parameters utilized in Differential Scanning Calorimetry analysis for the selected thermoplastic composite materials.*

Material	Heating Rate (°C/min)	Sample Pan	Max. Temperature (°C)	Sample Size (mg)	Purge flow rate (cm^3/min)	Heating mode
PETG	10	Aluminum	300	4.5	50	Ramp
PA 6/6	10	Aluminum	300	5.3	50	Ramp
PPS	10	Aluminum	330	5.1	50	Ramp

Scanning Electron Microscopy (SEM)

A finely focused electron beam is moved in a raster pattern over the specimen surface. A signal is excited by the electron beam, and this signal is measured by a detector which, depending on the signal strength, displays an array of points of varying brightness level that is interpreted by the viewer as an image.

During the moisture absorption test, flexural samples retained moisture thus low vacuum mode was necessary in order to maintain the sample´s integrity. As SEM works at high vacuum, the residue of the tested fluids could evaporate and damage the vacuum pumping system. In Table 4 a summary of the setup used for SEM imaging is shown.

Table 5. *Scanning Electron Microscopy parameters for low vacuum mode imaging.*

Vacuum	Low vacuum mode (0.6 Torr)
Spot Size	4.0
Voltage	20 kV
Gun Pressure	1.65 e^{-9} Torr
Emission Current	198 μA

Tensile Testing

Determining the tensile properties of the proposed materials was conducted according to ASTM D3039 (Standard Test Method for Tensile Properties of Polymer Matrix Composite Materials). A uniaxial servo-hydraulic load frame (810 Materials Test System) was utilized to perform tensile testing. Its loading capacity ranges from 25 kN to

500 kN. In order to preserve sample´s integrity and adequate transfer of the load, tabbing was used according to standard ASTM D3039. In Table 6, the utilized testing parameters for tensile testing are summarized.

Table 6. *Tensile testing parameters utilized according to ASTM D3039.*

Material	Loading Rate (mm/min)	Max Displacement (mm)
PETG	1.3	50
PA 6/6	1.3	50
PPS	1.3	50

According to ASTM standard D3039, the elastic modulus is calculated by plotting the stress and strain generated in the sample. In order to accurately record the strain experienced by the sample, a MTS 632.18E-20 diametral extensometer was used. In Figure 4, the setup utilized during tensile testing is shown.

Figure 4. *Tensile testing setup. MTS extensometer placed on the sample to record the strain during the testing.*

ASTM standard D3039 states that the calculation for tensile strength (σ) and tensile modulus (E) is computed as follows:

$$\sigma = {}^{P}/_{A}$$

$$E = \frac{\Delta\sigma}{\Delta\varepsilon}$$

Where:

P= Force (N)

A= Cross sectional area (mm^2)

$\Delta\sigma$=Difference in applied tensile strength

$\Delta\varepsilon$=Difference between two strain points

Compression Testing

The procedure to define the compressive properties of the proposed materials was conducted according to ASTM standard D6641 (Standard Test Method for Compressive Properties of Polymer Matrix Composite Materials Using a Combined Loading Compression Test Fixture). A uniaxial servo-hydraulic load frame (810 Materials Test System) was utilized to perform compression testing. Its loading capacity ranges from 25 kN to 500 kN. In order to preserve the sample´s integrity and adequate transfer of the load, tabbing was used according to standard ASTM D6641. In Figure 5, the utilized combined loading compression test fixture for compression testing is shown.

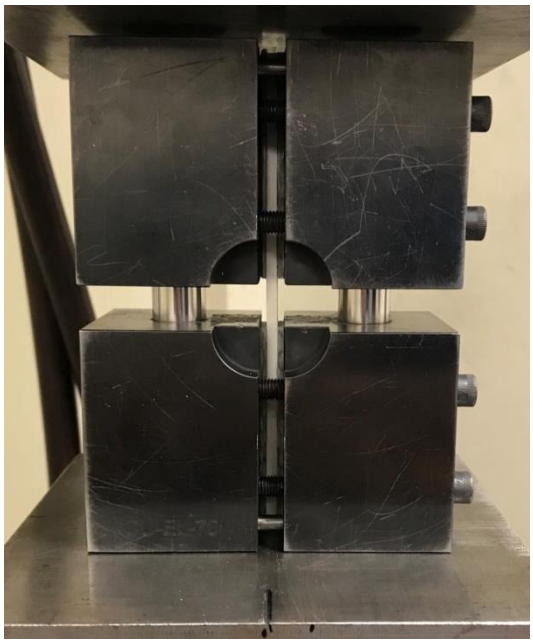

Figure 5. *Combined loading compression (CLC) test fixture utilized in unidirectional fiber composites compression testing.*

ASTM standard D6641 states that the calculations for compressive strength and compressive modulus are computed as follows:

$$\sigma = \frac{P_f}{wh}$$

$$E = \frac{\Delta\sigma}{\Delta\varepsilon}$$

Where:

P_f= Force (N)

w= Width (mm)

h= Thickness (mm)

$\Delta\sigma$=Difference in applied compressive strength

$\Delta\varepsilon$=Difference between two strain points

Flexural Testing

In order to determine the flexural properties of the proposed materials, flexural testing was conducted according to ASTM standard D790 (Standard Test Methods for Flexural Properties of Unreinforced and Reinforced Plastics and Electrical Insulating Materials). In Table 7, the utilized testing parameters for flexural testing are summarized. In Figure 6, the setup utilized for flexural testing is shown. A uniaxial servo-hydraulic load frame (858 Mini Bionix Materials Test System) was utilized to perform flexural testing. Its loading capacity ranges from 5 kN to 25 kN.

Table 7. *Flexural testing parameters utilized according to ASTM D790*

Material	Loading Rate (mm/min)	Span (mm)
PETG	1.1	40
PA 6/6	1.2	45
PPS	1.25	50

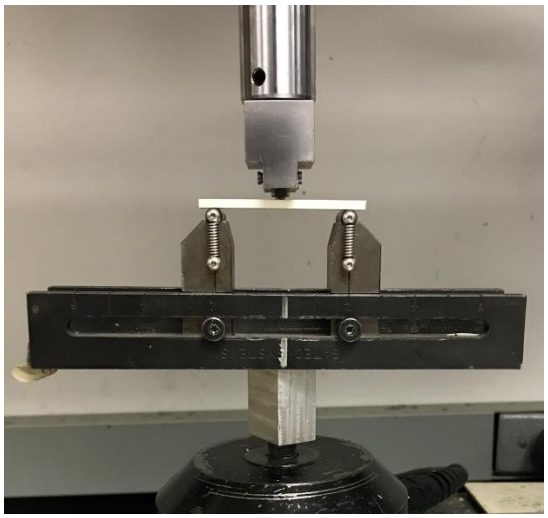

Figure 6. *Utilized setup for flexural testing according to ASTM standard D790.*

ASTM standard D790 states that the calculations for flexural strength and flexural modulus are computed as follows:

$$\sigma = \frac{3PL}{2bd^2}$$

$$E = \frac{L^3 m}{4bd^3}$$

Where:

σ= Stress (MPa)

E= Modulus of elasticity (GPa)

P= Load at given point (N)

L= Support span (mm)

b= Width of beam tested (mm)

d= Depth of beam tested (mm)

m= Slope of the tangent to the initial straight-line portion of the load-deflection curve (N/mm)

Shear Testing

The procedure to define the shear properties of the proposed materials was conducted according to ASTM standard D5379 (Standard Test Method for Shear Properties of Composite Materials by the V-Notched Beam Method). A uniaxial servo-hydraulic load frame (810 Materials Test System) was utilized to perform shear testing. Its loading capacity ranges from 25 kN to 500 kN. In Figure 7, the setup and fixture utilized for flexural testing is shown.

Figure 7. *V-Notched beam test fixture required to perform shear testing of composite materials according to ASTM standard D537.*

ASTM standard D5379 states that the calculations for shear strength (σ^u) and shear modulus (G) are computed as follows:

$$\sigma^u = \frac{P^u}{wh}$$

$$G = \frac{\Delta\tau}{\Delta\gamma}$$

Where:

P^u= Force (N)

w= Width at notched section (mm)

h= Thickness at notched section (mm)

$\Delta\tau$= Difference in applied shear strength between two points

$\Delta\gamma$= Difference between two strain points

Moisture Absorption

In order to determine the moisture response of the proposed materials, moisture absorption testing was conducted according to ASTM standard D5229 (Standard Test Method for Moisture Absorption Properties and Equilibrium Conditioning of Polymer Matrix Composite Materials). When working with fluids with an unknown Diffusion Coefficient, ASTM D5229 states that samples must be fully submerged in each fluid for no less than 7 days (168 h). Weight and dimensional change was recorded on a daily

basis utilizing a 0.1 μg resolution lab scale. It is critical to mention that all samples were oven dried at 200°F for a span of 24 hours before its first weight record.

Each fluid was kept in individual closed containers in which three flexural samples of each material were submerged as shown in Figure 8. In Table 8, a description of the considered fluids for this testing is provided.

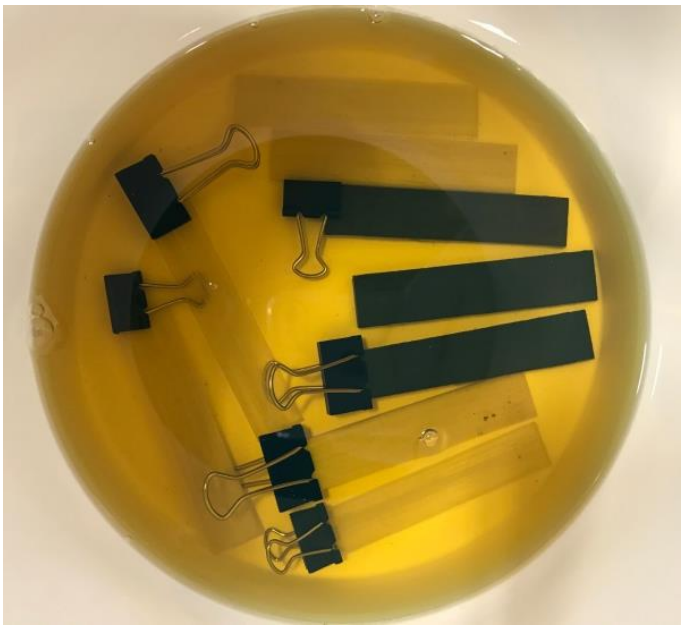

Figure 8. *Individual closed container in which the samples were kept during the testing.*

Table 8. *Considered fluids for the liquid absorption testing.*

Fluid Type	Specifications
Water	@ Room temperature
Brine	23% NaCl (Ice away Rock Salt), 77% water
Gasoline	Chevron Regular (87 octanes)
Diesel	Chevron 2-D
Motor Oil	Quaker State SAE 10W-30 Synthetic Blend
Used Motor Oil	Quaker State SAE 10W-30 Synthetic Blend after 3,000 miles
Brake Fluid	Prestone DOT 3 High Temperature Synthetic
Anti-Freeze	Prestone 50/50 Prediluted
Automatic Transmission Fluid	Castrol Transmax DEX/MERC

ASTM standard D5229 requires that the calculation for the moisture absorption of laminated composite materials must be made as follows:

$$M, \% = \frac{W_i - W_0}{W_0}$$

Where:

$M, \%$= Moisture absorption (%)

W_i= Sample weight after exposure (g)

W_0= Sample weight before exposure (g)

Degree of Crystallinity

Depending on polymer structure, polymers can be either semi-crystalline or amorphous. The degree of crystallinity in thermoplastics depends on several factors such as molecular weight, molecular architecture (side group size), polymer chain length, etc. (Chawla, 2012).

The degree of crystallinity in polymer is calculated as follows:

$$X_c = \left(\frac{(\Delta H_m - \Delta H_{cc})}{\Delta H_c}\right) x\ 100$$

Where:

X_c= Degree of crystallinity (%)

ΔH_m= Heat of fusion (J/g)

ΔH_{cc}= Heat of cold crystallization (J/g)

ΔH_c= Heat of fusion for 100% crystalline polymer (J/g)

The heat of fusion and heat of cold crystallization can be obtained by integrating the areas under the curve generated by differential scanning calorimetry. Whereas heat of fusion for a 100% crystalline polymer is a theoretical value since 100% crystalline polymers are hardly found, the ability of a polymer to form crystals is strongly correlated to the entanglement of polymeric chains that never can undergo the reorganization necessary to create a fully crystalline state.

3. RESULTS

Define a Suitable Glass Fiber Reinforced Thermoplastic for Leaf Spring Application.

The main driver of this research is the application of the results from an industrial point of view; production cost and time are the most important variables. It is important to mention that the cost for thermoplastic materials is strongly related to the production volume. A material such as Polyetheretherketone (PEEK) has very attractive properties, but its low production volume makes its applications very limited (Jones & Leach, 1993). Therefore, three different thermoplastic materials were investigated: Polyethylene Terephthalate Glycol (PETG), Polyamide 6/6 (PA/66) and Polyphenylene Sulfide (PPS). These materials are reinforced with continuous E-glass fiber.

Tensile Properties

Tensile testing of the three glass fiber reinforced thermoplastic materials was performed to compare both tensile strength and tensile modulus in the 0° fiber orientation and 90° fiber orientation. Five samples of each material and fiber orientation were tested, and the comparison is shown in Figure 9.

Tensile properties in the 0° direction are closely affected by the fiber weight content of the composite. If we compare the matrices alone, PETG would show significantly lower properties that PPS and PA 6/6. In this case, PETG has 5% more fiber than PA 6/6 and

PPS, shows similar properties in the 0° fiber orientation; whereas in 90° fiber orientation, PPS shows higher tensile strength and modulus as PETG and PA 6/6. In the 90° fiber orientation samples, most of the load is being handled by the resin without any extra reinforcement from the fibers. It is expected that the higher UTS will be shown by PPS.

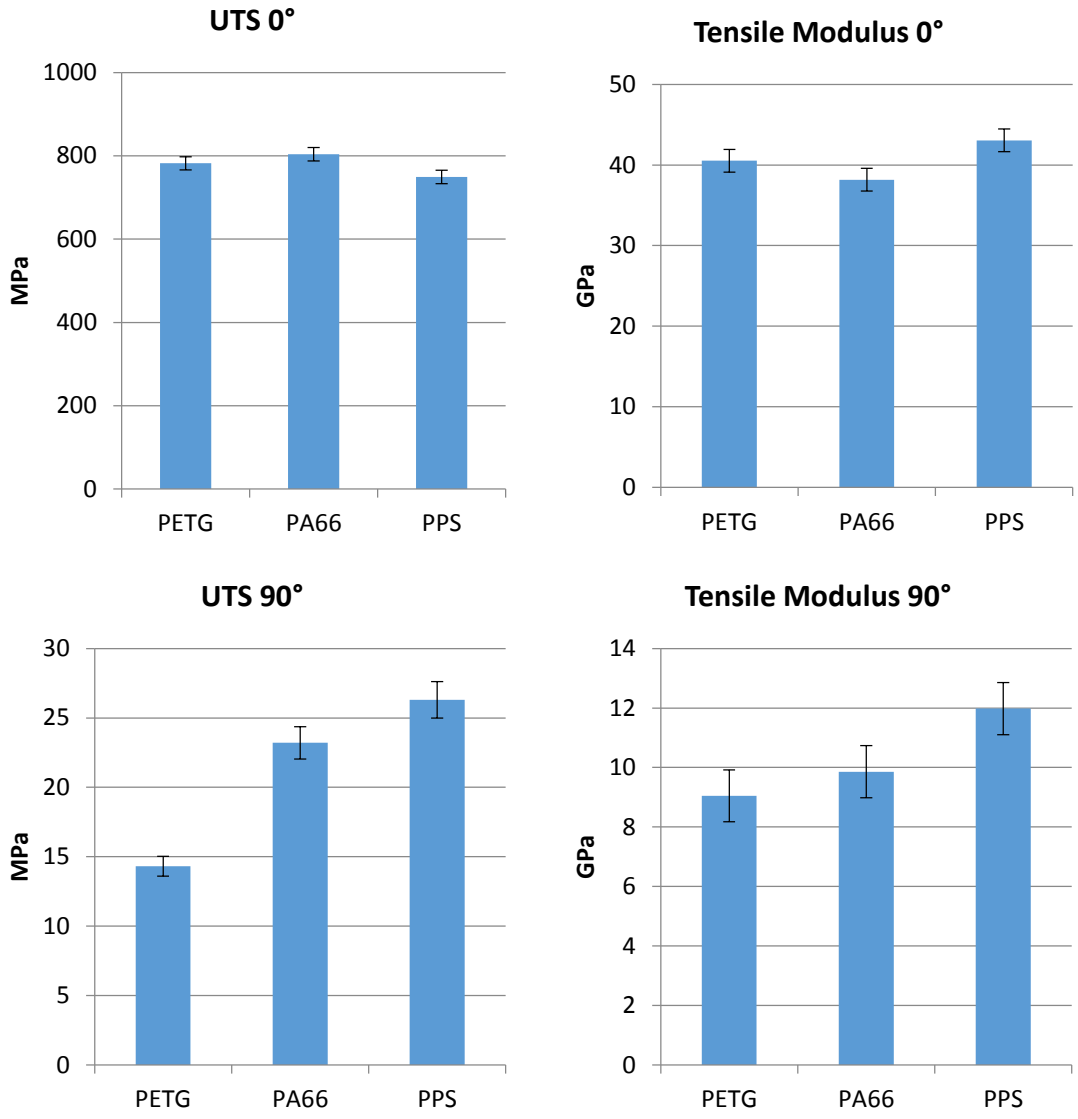

Figure 9.*Tensile strength and modulus comparison between PETG, PA 6/6 and PPS for unidirectional fiber orientation at 0° and 90°.*

In composites, three elements should be taken into account when studying its mechanical properties: fiber strength, matrix strength and bonding strength. According to the literature, neat PPS exhibits a higher tensile strength than neat PA 6/6 (Harper, 2004). Interface strength has an important impact on the mechanical performance of the composite. In Figure 10, a scanning electron microscopy (SEM) imaging is shown of a tested PPS tensile sample in the 0° fiber orientation. Figure 11 shows a SEM image of a PA 6/6 tensile sample in the 0° fiber orientation. Comparing both images, it can be detected that PA 6/6 creates a strong interface between fiber and matrix. PPS on the other hand, showed a poor fiber-matrix interface compared with PA 6/6.

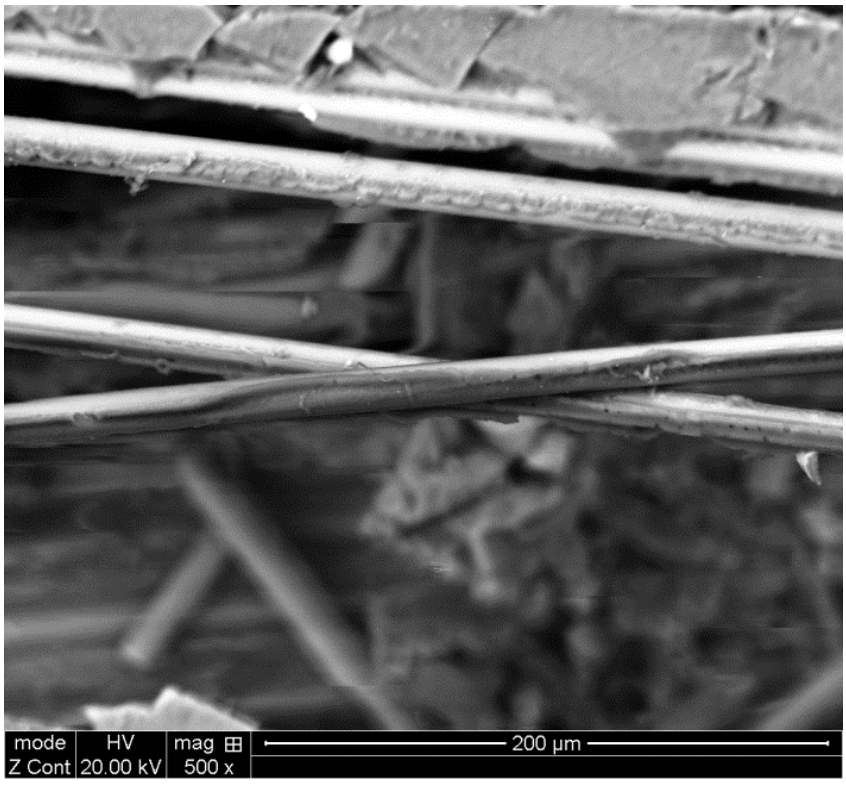

Figure 10. *Fiber-Matrix SEM imaging of a tensile tested PPS sample with fiber orientation at 0°.*

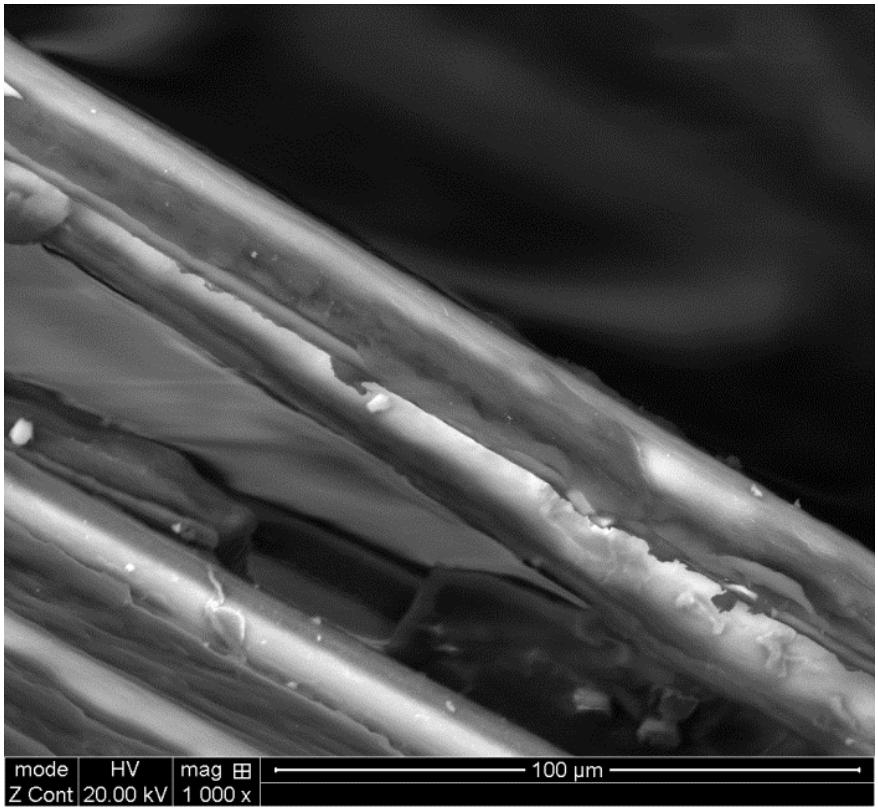

Figure 11.*Fiber-Matrix SEM imaging of a tensile tested PA 6/6 sample with fiber orientation at 0°.*

Compressive Properties

Compression testing of the three glass fiber reinforced thermoplastic materials was performed to compare both compressive strength and compressive modulus in the 0° fiber orientation and 90° fiber orientation. Five samples of each material and fiber orientation were tested, and the comparison is shown in Figure 12.

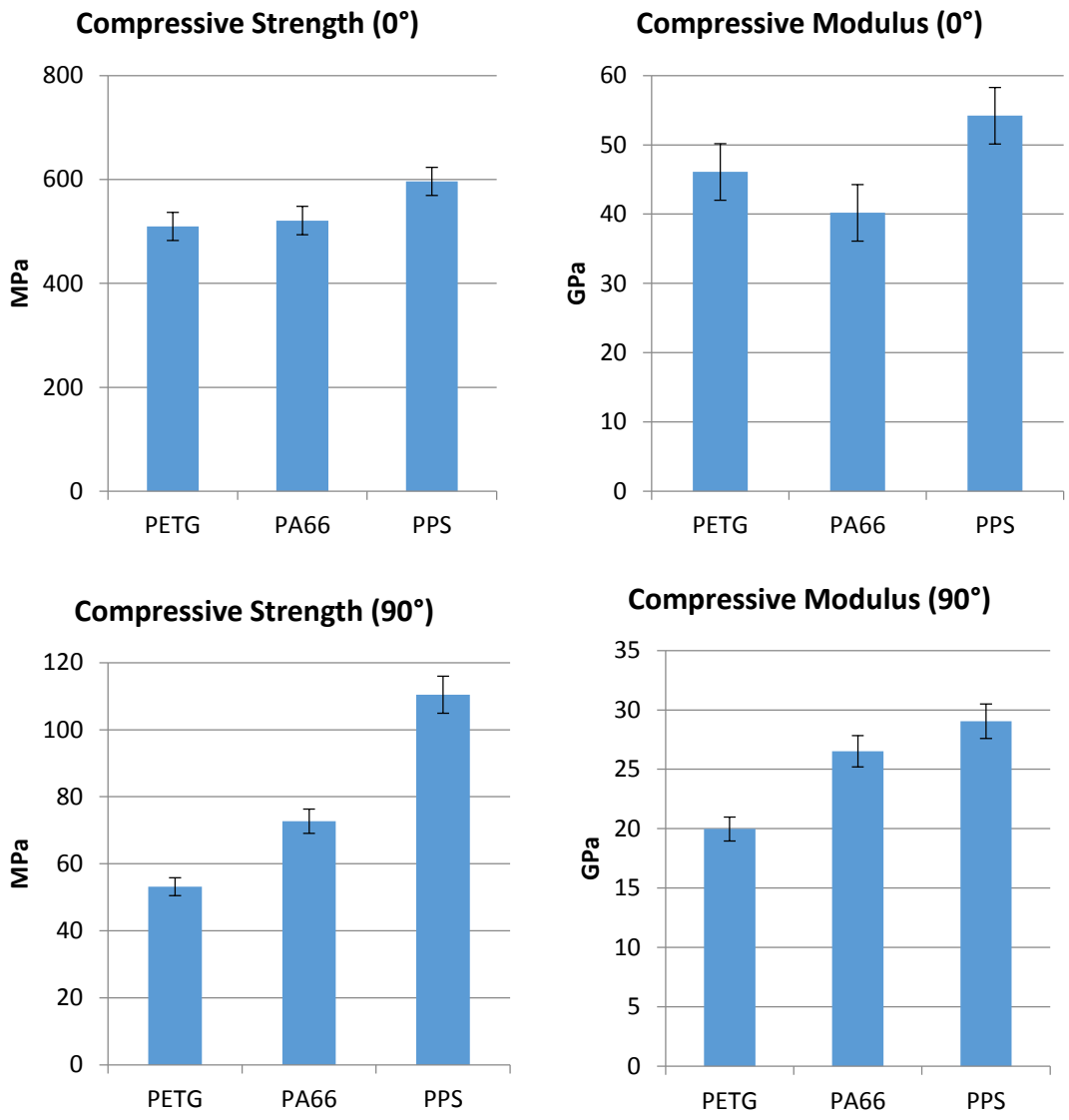

Figure 12. *Compressive strength and compressive modulus comparison between PETG, PA 6/6 and PPS for unidirectional fiber orientation at 0° and 90°.*

Comparable with tensile results showed above, higher compressive properties in both 0° and 90° fiber orientation are showed by PPS. Compressive properties just like tensile properties are closely related to fiber weight content present in the composite.

Flexural Properties

Compression testing of the three glass fiber reinforced thermoplastic materials was performed to compare both compressive strength and compressive modulus in the 0° fiber orientation and 90° fiber orientation. Five samples of each material and fiber orientation were tested, and the comparison is shown in Figure 13.

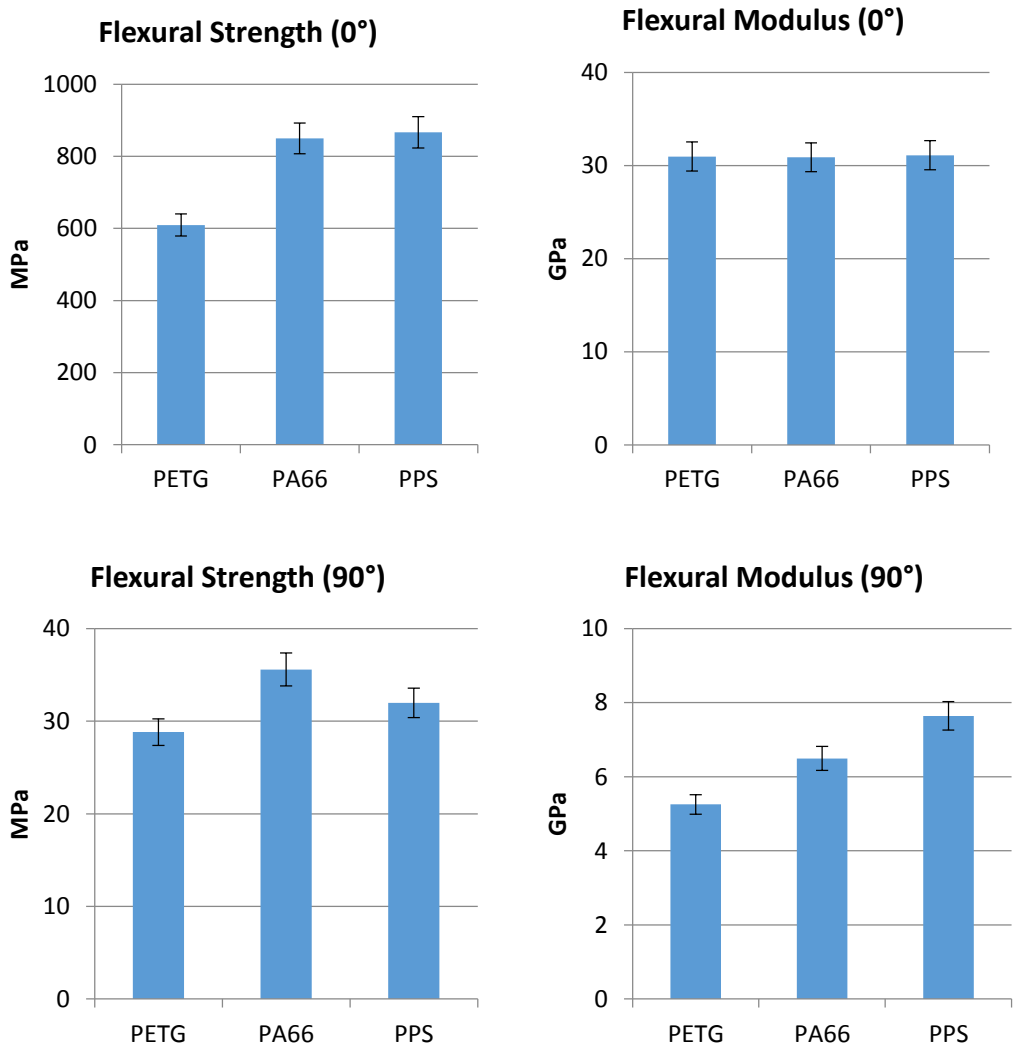

Figure 13. *Flexural strength and flexural modulus comparison between PETG, PA 6/6 and PPS for unidirectional fiber orientation at 0° and 90°.*

Shear Properties

Compression testing of the three glass fiber reinforced thermoplastic materials was performed to compare both compressive strength and compressive modulus in the 0° fiber orientation and 90° fiber orientation. Five samples of each material and fiber orientation were tested, and the comparison is shown in Figure 14.

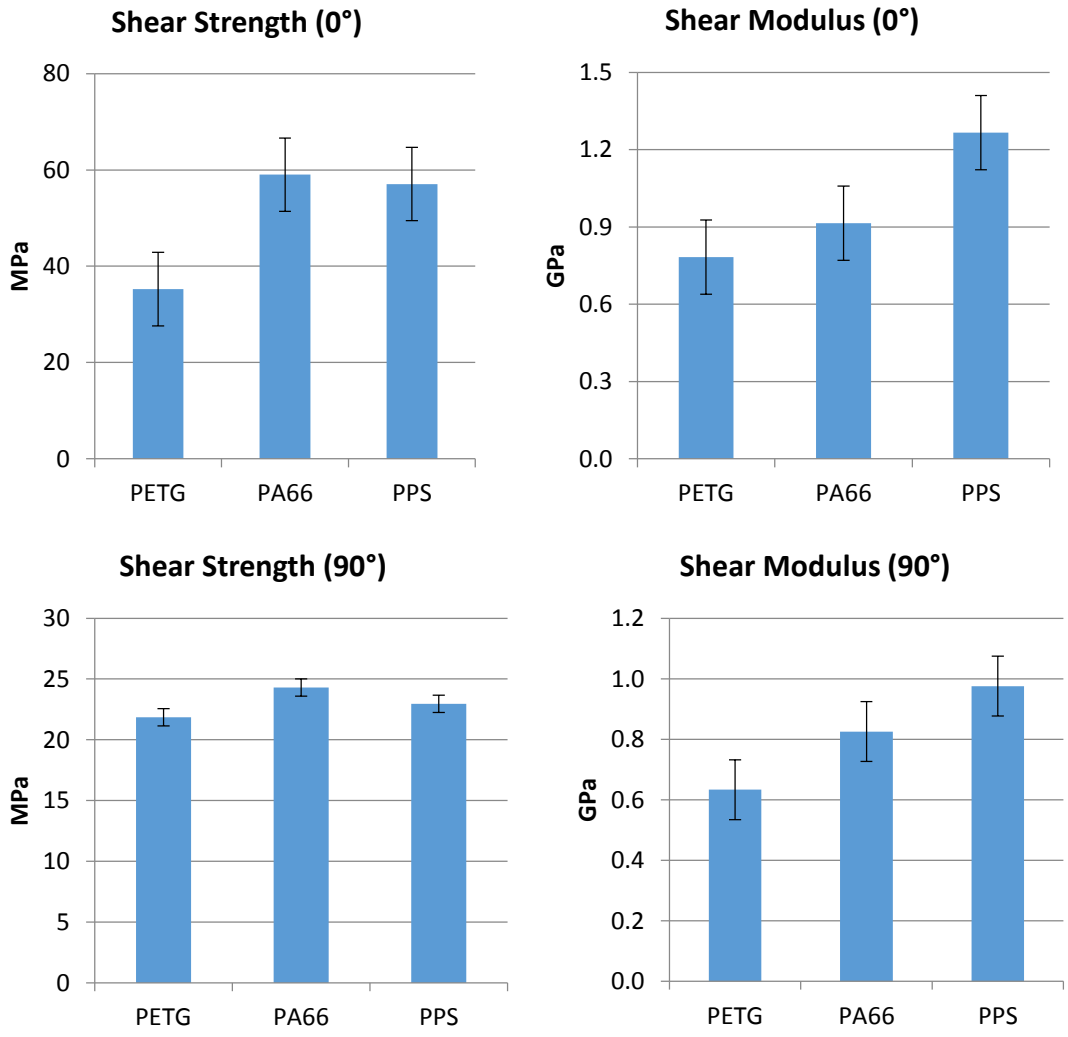

Figure 14. *Shear strength and shear modulus comparison between PETG, PA 6/6 and PPS for unidirectional fiber orientation at 0° and 90°.*

Moisture Absorption

The rate at which a certain fluid is absorbed by a composite depends on many material variables: the type of fiber, the type of matrix, fiber orientation with respect to the direction of diffusion, the temperature, the difference in moisture concentration between the composite and the environment and whether the absorbed fluid reacts chemically with the matrix. (Valentin, 1987).

During its lifetime, a leaf spring will be exposed to a number of different fluids and substances. Nine different automotive fluids were considered for this analysis. The main goal of this experiment is to determine if the composite is going to experiment considerable dimensional changes (swelling, delamination, etc.) and if their original mechanical properties would be affected by the continuous exposure to such fluids. Two different fiber orientation samples were tested: 0° and 90°. According to ASTM D5229, samples were maintained submerged for 7 days, recording their weight change every 24 hours.

Fluid Absorption (0° Samples)

In Figure 15, a summary of the weight variation results for each of the nine fluids and the three thermoplastic composites samples in the 0° fiber orientation is shown.

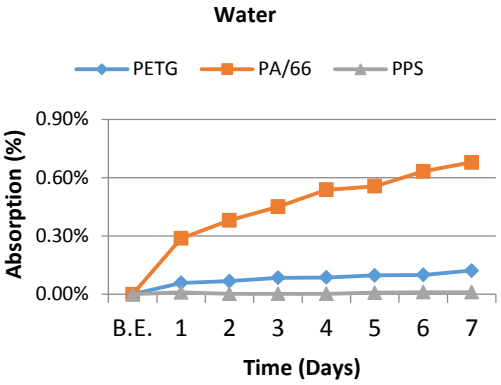
Water
PETG
PA/66
PPS
0.90%
0.60%
0.30%
0.00%
Absorption (%)
B.E. 1 2 3 4 5 6 7
Time (Days)

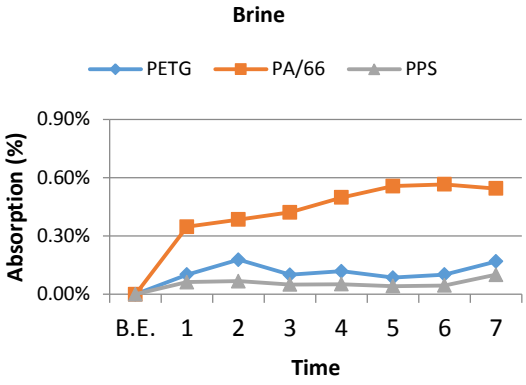
Brine
PETG
PA/66
PPS
0.90%
0.60%
0.30%
0.00%
Absorption (%)
B.E. 1 2 3 4 5 6 7
Time

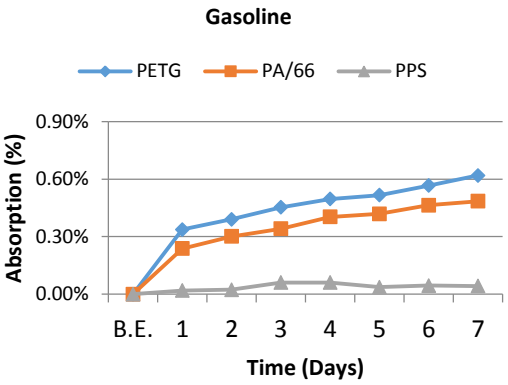
Gasoline
PETG
PA/66
PPS
0.90%
0.60%
0.30%
0.00%
Absorption (%)
B.E. 1 2 3 4 5 6 7
Time (Days)

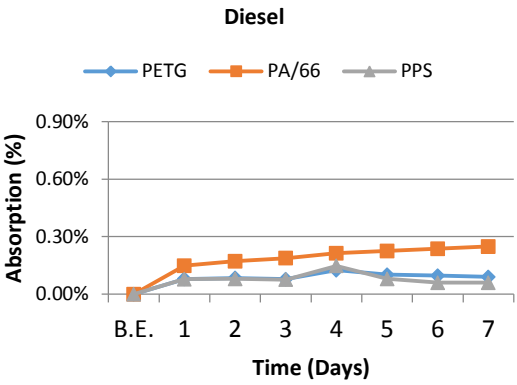
Diesel
PETG
PA/66
PPS
0.90%
0.60%
0.30%
0.00%
Absorption (%)
B.E. 1 2 3 4 5 6 7
Time (Days)

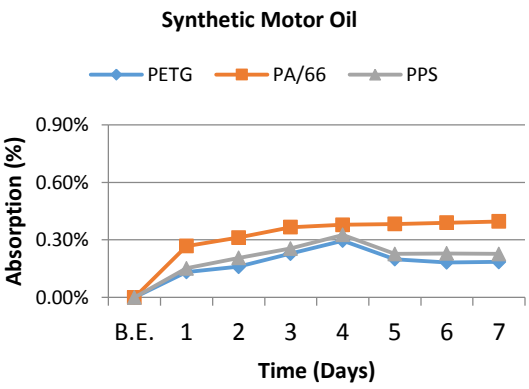
Synthetic Motor Oil
PETG
PA/66
PPS
0.90%
0.60%
0.30%
0.00%
Absorption (%)
B.E. 1 2 3 4 5 6 7
Time (Days)

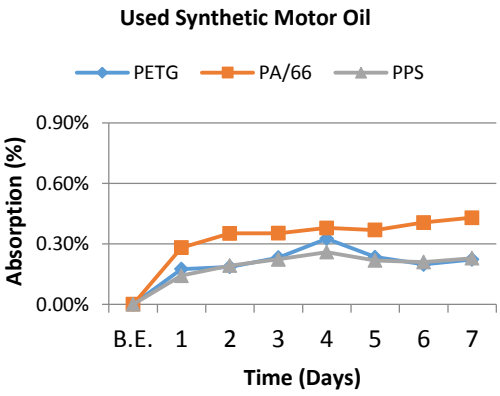
Used Synthetic Motor Oil
PETG
PA/66
PPS
0.90%
0.60%
0.30%
0.00%
Absorption (%)
B.E. 1 2 3 4 5 6 7
Time (Days)

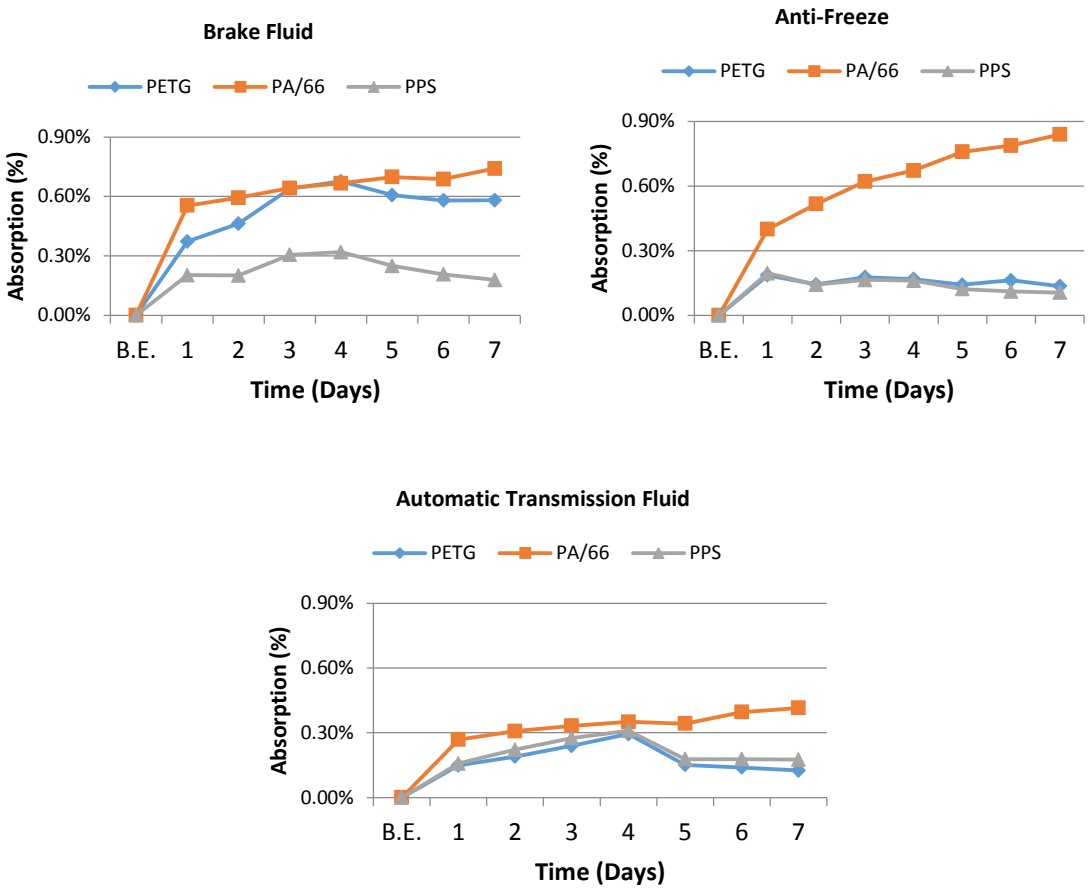

Figure 15. *PETG, PA6/6 and PPS liquid absorption comparison for nine different automotive fluids after 7 day exposure. Unidirectional 0° fiber orientation samples.*

Fluid Absorption (90° Samples)

In Figure 16, a summary of the weight variation results for each of the nine fluids and the three thermoplastic composites samples in the 90° fiber orientation is shown.

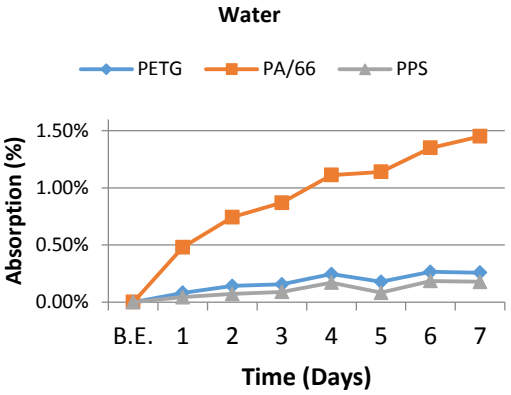
Water
PETG
PA/66
PPS
Absorption (%)
1.50%
1.00%
0.50%
0.00%
B.E. 1 2 3 4 5 6 7
Time (Days)

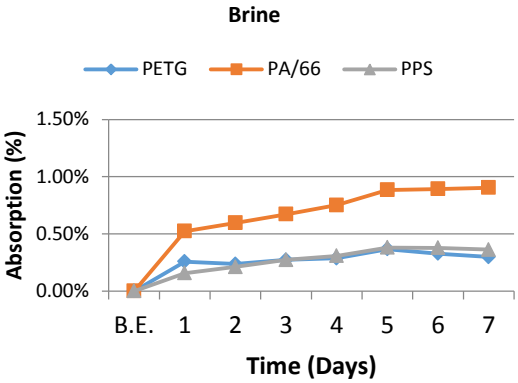
Brine
PETG
PA/66
PPS
Absorption (%)
1.50%
1.00%
0.50%
0.00%
B.E. 1 2 3 4 5 6 7
Time (Days)

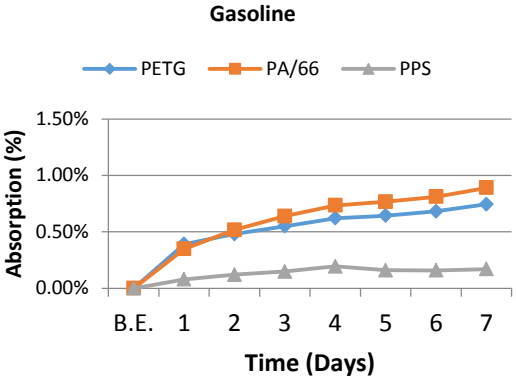
Gasoline
PETG
PA/66
PPS
Absorption (%)
1.50%
1.00%
0.50%
0.00%
B.E. 1 2 3 4 5 6 7
Time (Days)

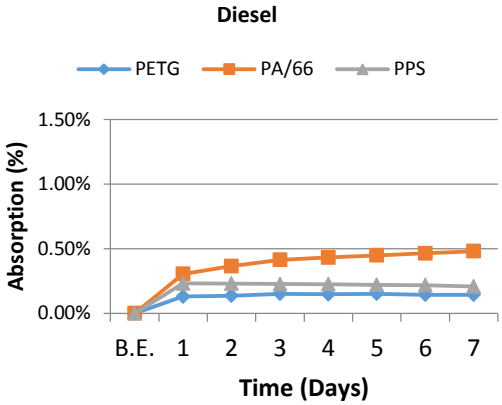
Diesel
PETG
PA/66
PPS
Absorption (%)
1.50%
1.00%
0.50%
0.00%
B.E. 1 2 3 4 5 6 7
Time (Days)

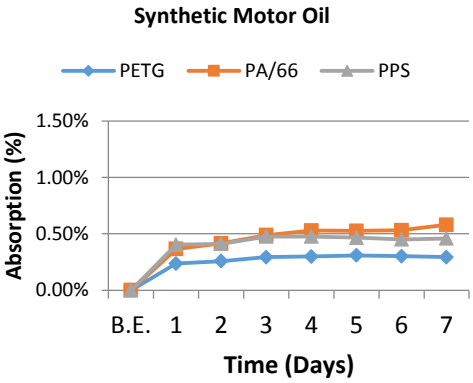
Synthetic Motor Oil
PETG
PA/66
PPS
Absorption (%)
1.50%
1.00%
0.50%
0.00%
B.E. 1 2 3 4 5 6 7
Time (Days)

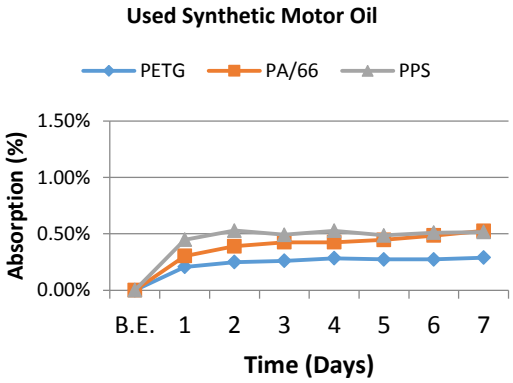
Used Synthetic Motor Oil
PETG
PA/66
PPS
Absorption (%)
1.50%
1.00%
0.50%
0.00%
B.E. 1 2 3 4 5 6 7
Time (Days)

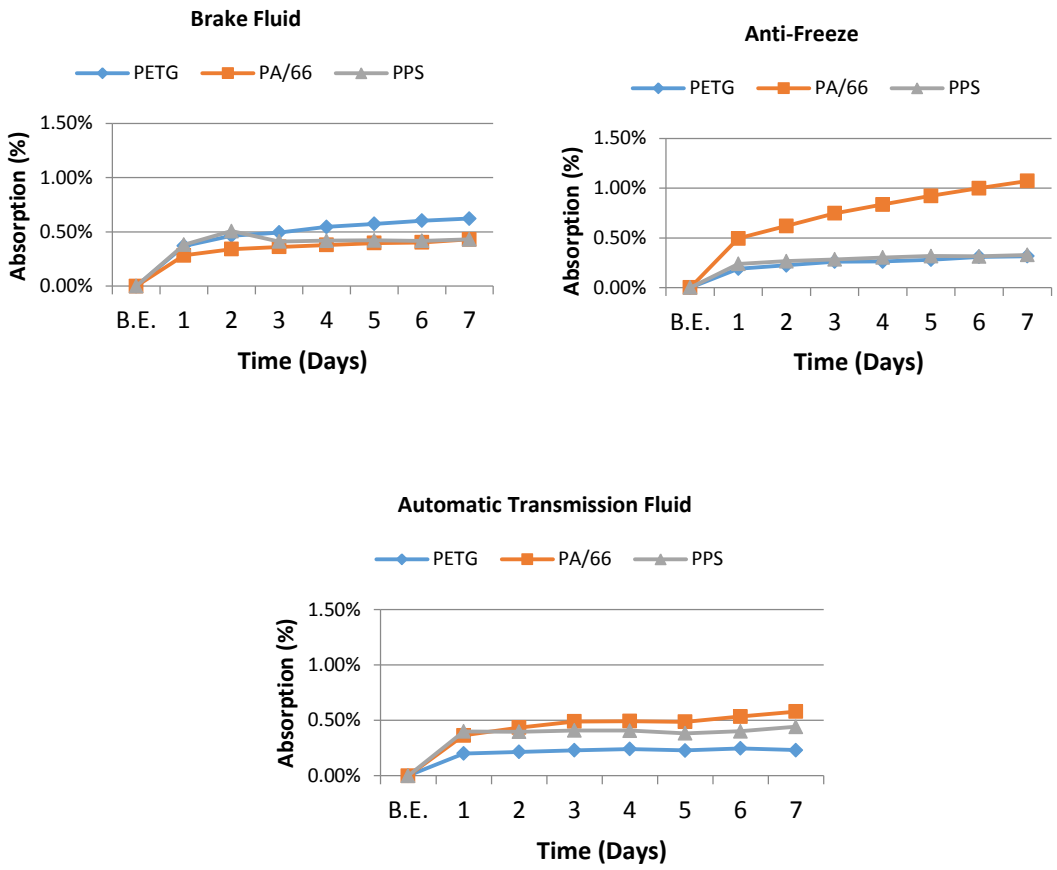

Figure 16. *PETG, PA6/6 and PPS liquid absorption comparison for nine different automotive fluids after 7 day exposure. Unidirectional 90° fiber orientation samples.*

After analyzing the data, it is evident that PA 6/6 composite showed a higher hydrophilic behavior compared with PPS and PETG composites for both 0° and 90° fiber orientations. Leaf spring application will require the selected material to be exposed to a variety of conditions that may include any of these automotive fluids. PPS shows the best stability after the exposure followed by PETG. In the automotive industry, dimensional stability in structural components is highly demanded; and low variation during the lifetime of a component is highly expected.

Flexural Strength after Exposure

Flexural samples at 0° and 90° fiber orientation were tested after being exposed in nine different automotive fluids. The flexural strength of each thermoplastic composite sample was compared with a flexural sample not exposed to any of the analyzed fluids in order to determine the effect of the each fluid on the composite´s mechanical performance. In Figure 17, 18 and 19 a summarized plot of the flexural strength after moisture exposure is shown for PETG, PA 6/6 and PPS respectively.

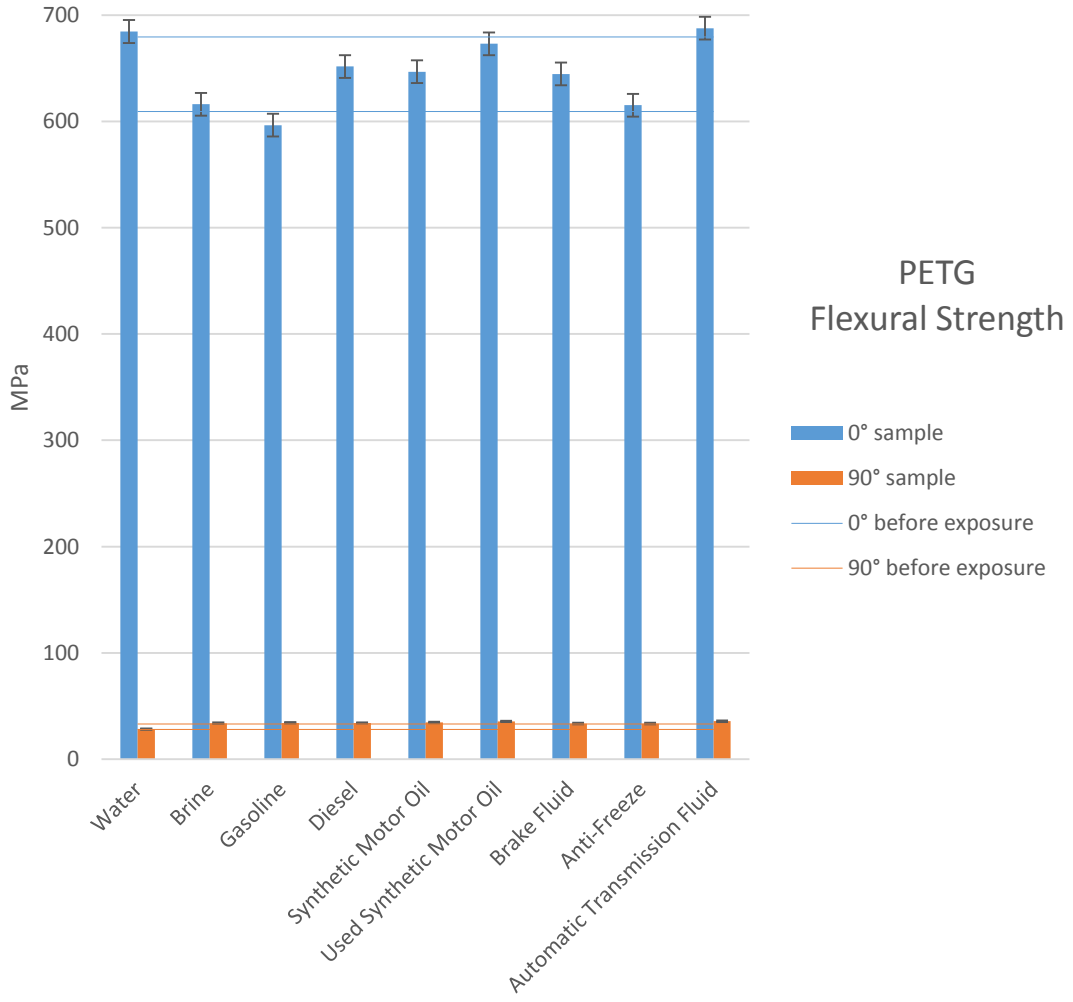

Figure 17.*Flexural strength of PETG/GF composite after 7 day exposure to automotive fluids. Samples (0° and 90°) are compared with unexposed PETG.*

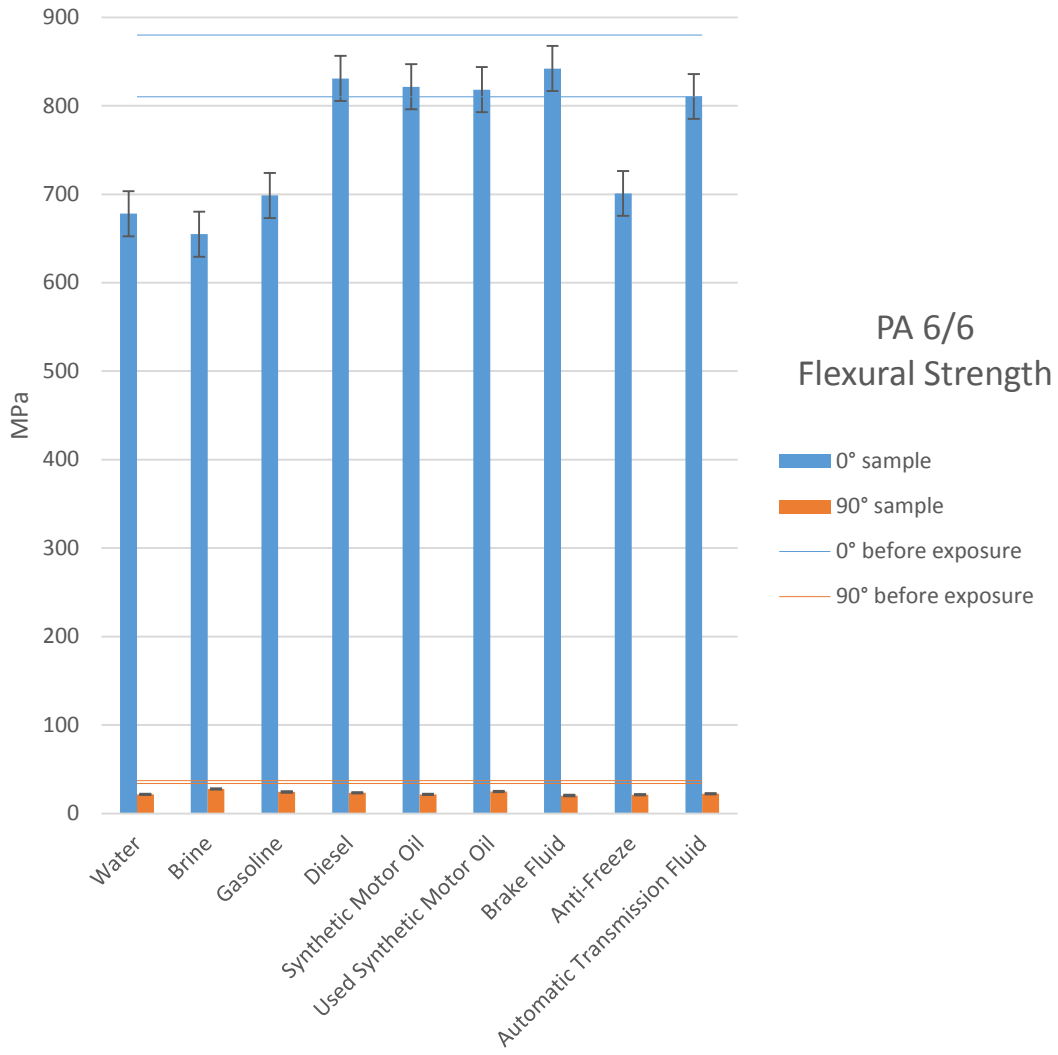

Figure 18.*Flexural strength of PA 6/6/GF composite after 7 day exposure to automotive fluids. Samples (0° and 90°) are compared with unexposed PA 6/6.*

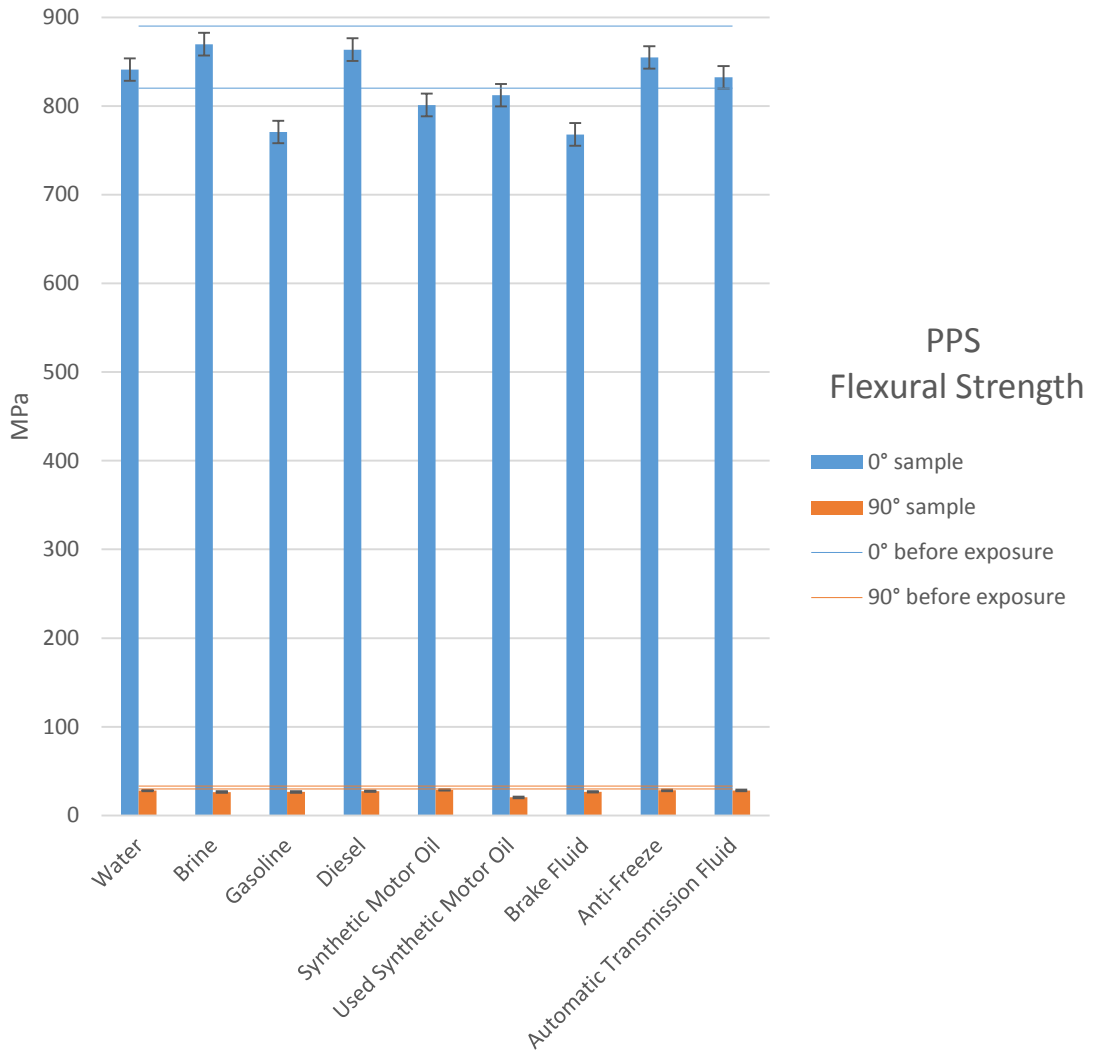

Figure 19.*Flexural strength of PPS/GF composite after 7 day exposure to automotive fluids. Samples (0° and 90°) are compared with unexposed PPS.*

Figure 17 shows that after 7 days of exposure PETG has not changed its flexural properties except by a slight increase when exposed to water, diesel, both used and not used synthetic motor oil, and automatic transmission fluid.

Two different property degradation mechanisms are considered in this experiment: matrix plasticization and hydrolyzation of the fiber-matrix bond. Plasticization refers to a low molecular weight compound dissolving in a polymer (Juska, 1993).

Flexural Modulus after Exposure

Flexural samples at 0° and 90° fiber orientation were tested after being exposed in nine different automotive fluids. The flexural modulus of each composite sample was compared with a flexural sample not exposed to any of the analyzed fluids to determine the effect of the selected fluid on the composite mechanical performance. Figure 20 shows the effect that automotive fluids had on PETG flexural samples.

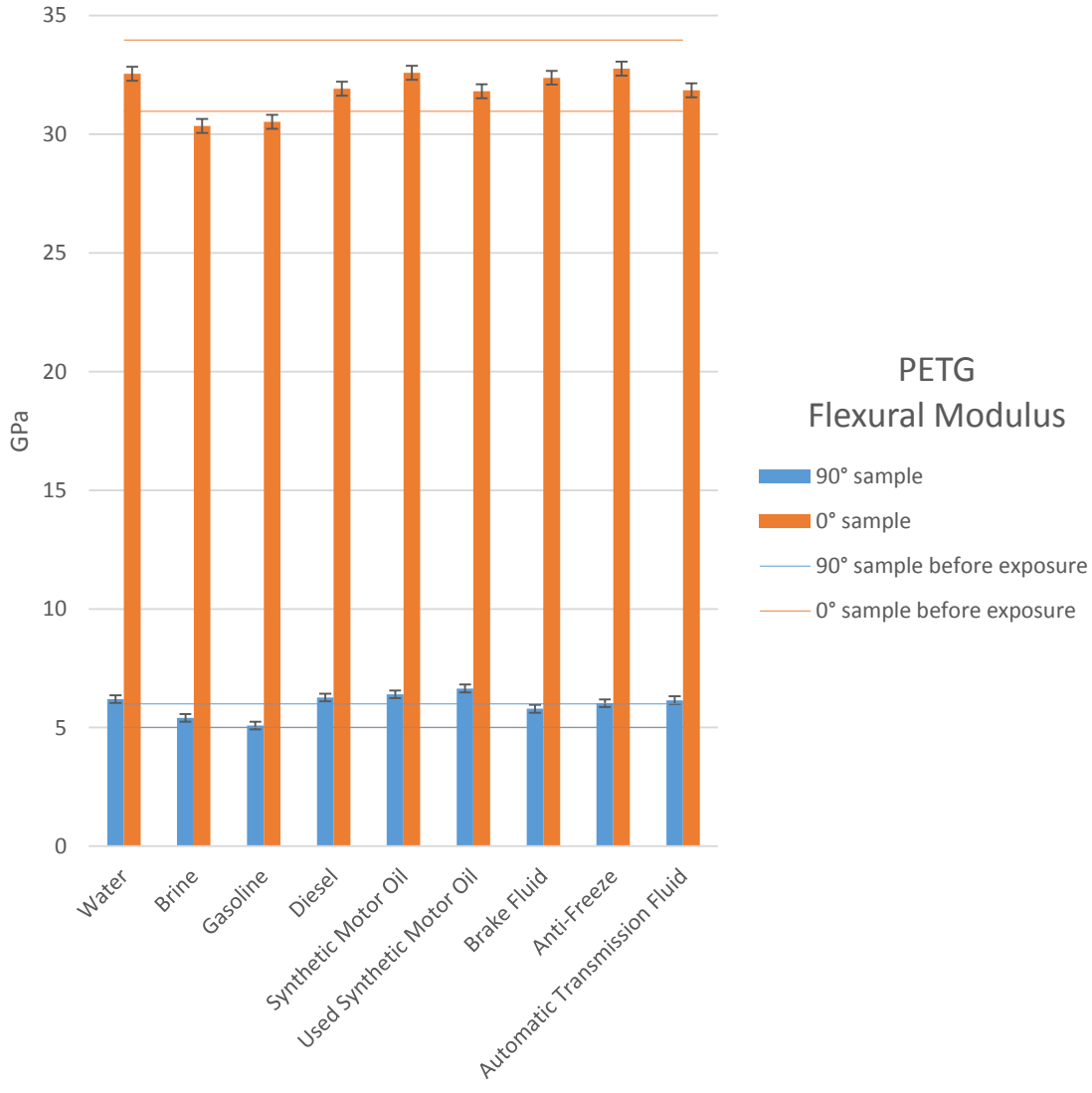

Figure 20. *Flexural Modulus of PETG/GF composite after 7 day exposure to automotive fluids. Samples (0° and 90°) are compared with unexposed PETG.*

Figure 21 shows the effect that automotive fluids had on PA 6/6 flexural samples. All nine fluids had an important effect on the flexural properties of PA 6/6 in both 0° and 90° fiber orientation.

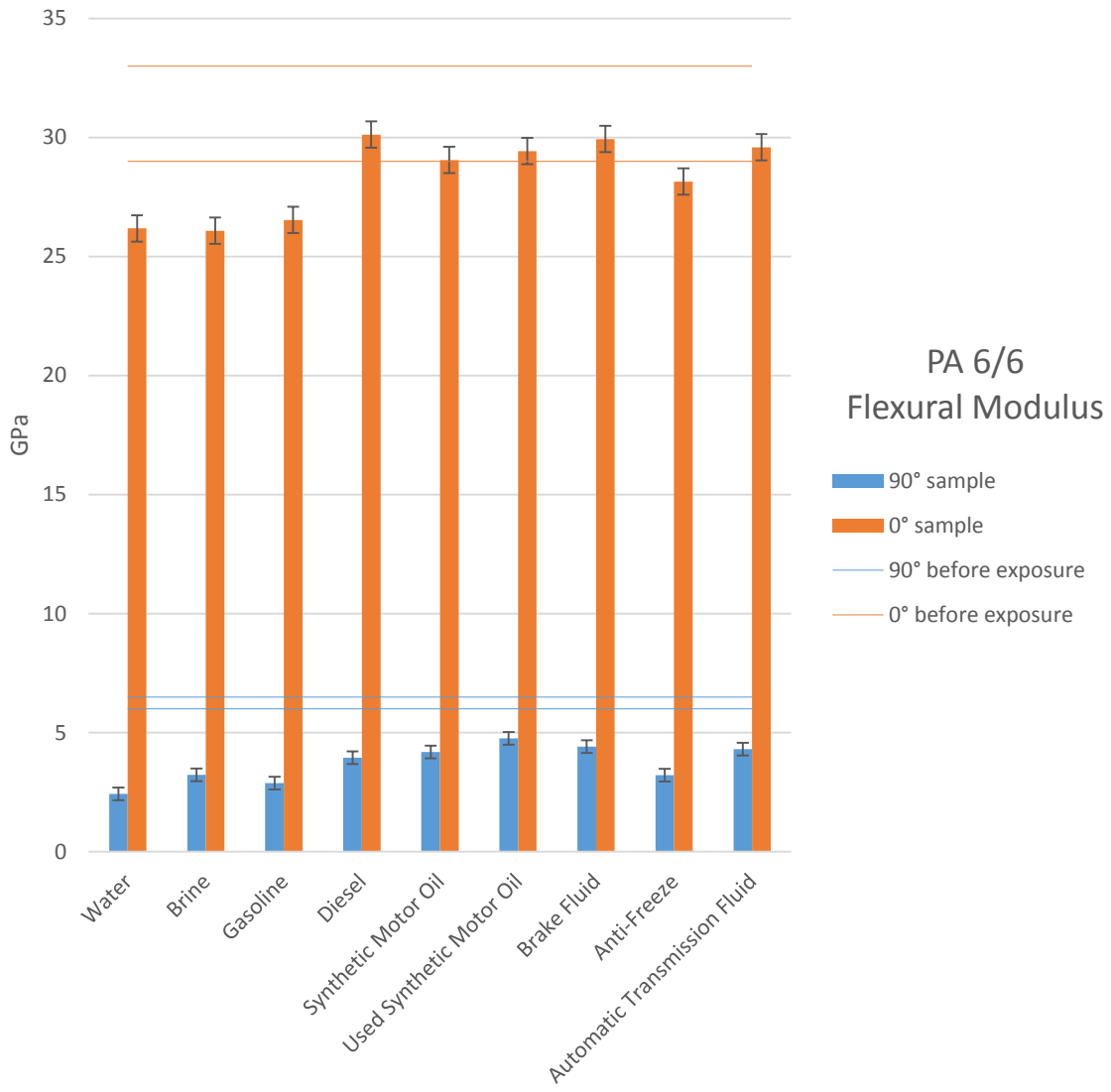

Figure 21. *Flexural Modulus of PA 6/6/GF composite after 7 day exposure to automotive fluids. Samples (0° and 90°) are compared with unexposed PA 6/6.*

As previously discussed, PA 6/6 has greater susceptibility to hydrolytic degradation as the other two investigated thermoplastic matrices. As shown in Figure 22, matrix residue

in fibers after testing appears to be degrading by continuous exposure to gasoline. This directs the attention of this problem to the matrix integrity instead of the fiber/matrix itself.

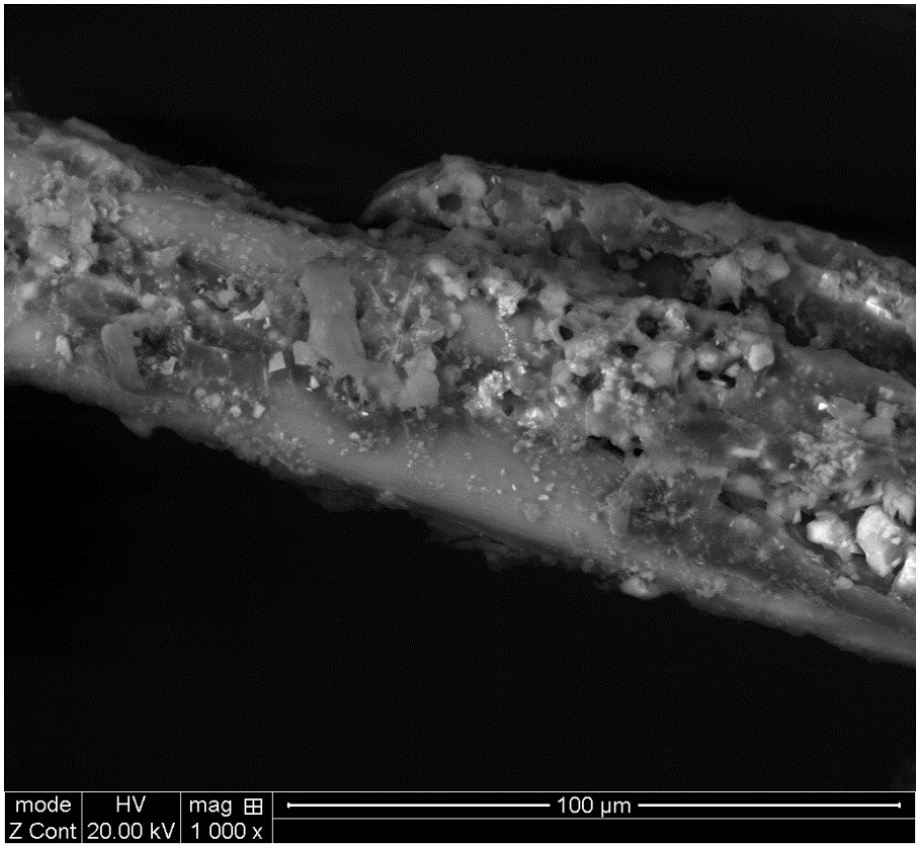

Figure 22. *Fiber-Matrix interface of a gasoline exposed PA 6/6 sample.*

Figure 23 shows the effect that automotive fluids had on PPS flexural samples. It is clearly noticed that all of the investigated fluids have a greater impact on the 90° fiber orientation samples that those of 0° fiber orientation.

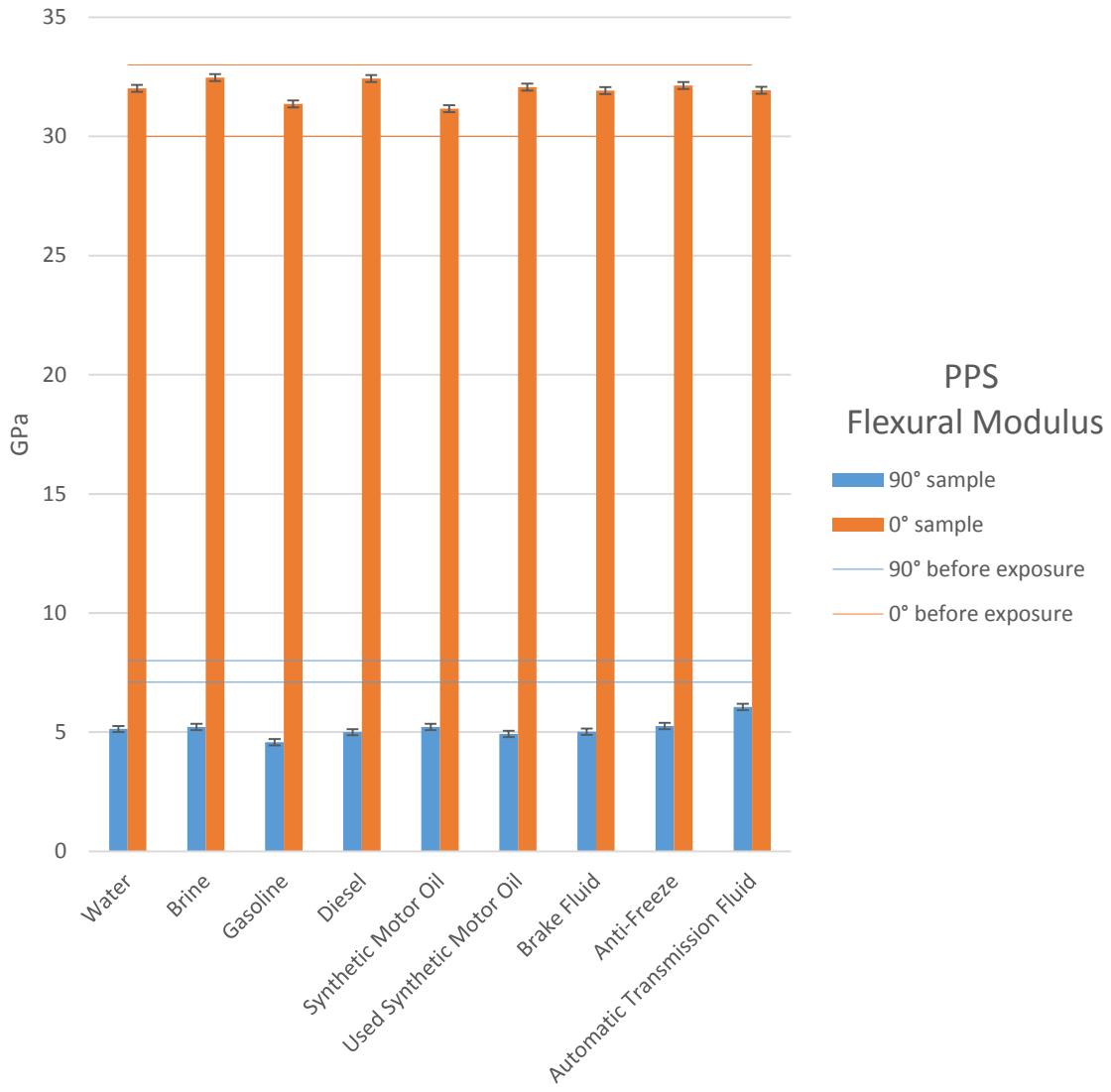

Figure 23. *Flexural Modulus of PPS/GF composite after 7 day exposure to automotive fluids. Samples (0° and 90°) are compared with unexposed PPS.*

Figure 24 shows the fracture surface of a 90° fiber orientation PPS flexural sample which was exposed for 7 days to brake fluid. It can be seen that the fluid had a considerable impact in the fiber/matrix interface since no residue is visible in the fibers in this particular region.

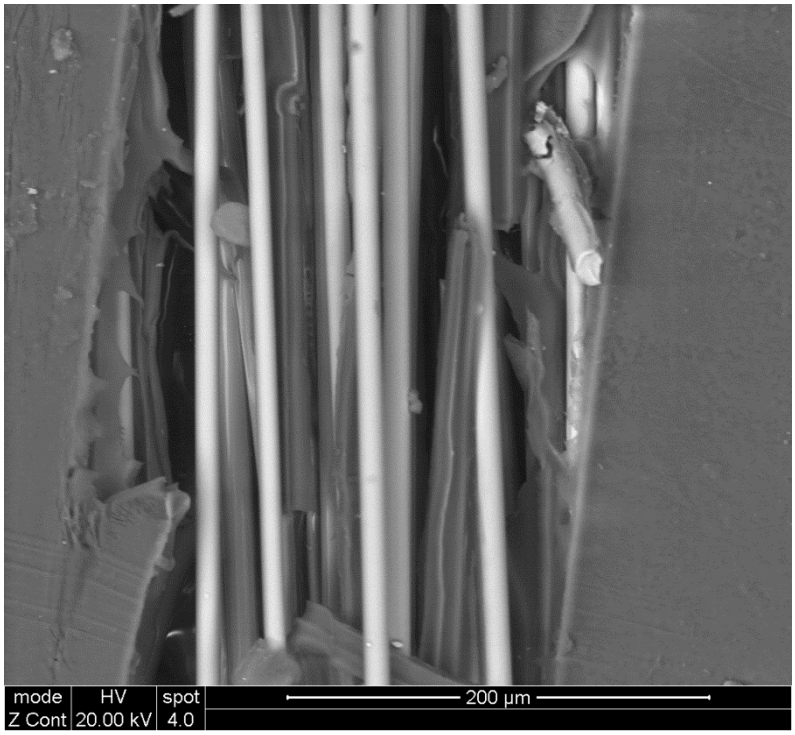

Figure 24. *Fracture surface of a PPS sample after being exposed to brake fluid for a period of 7 days.*

Just like in the 0° fiber orientation samples, matrix plasticization and hydrolyzation of the fiber-matrix bond are the two main mechanisms considered to be affecting the mechanical properties of the submerged samples. Work done by Lou, et. al, showed that PPS after exposure to water presented a sharp decrease in its mechanical properties and then stabilizing over time. It could also show that in long fiber thermoplastics (LFT) this loss of properties was lower than in continuous fiber composites. This indicated that the fiber matrix interface is affected by exposure to fluids (Lou, 1988).

Some considerations must be made when analyzing diffusion in unidirectional fiber composites. It must be taken into account that the diffusion coefficient of the matrix will change depending on the arrangement of fibers as well as the diffusion rate depending on whether or not the matrix has suffered plasticization. The diffusion rate will be strongly

affected by the orientation of the fibers in composites (Joliff, 2012). In Figure 25, Diffusion Direction A and B is shown. In Direction B, the unidirectional fibers simulate a barrier effect which will reduce the diffusion rate of the analyzed fluid. Whereas in Direction A, diffusion rate is significantly higher since the fibers do not create a high resistance path. This can be clearly identified in the amount of moisture absorbed by comparing two PA 6/6 samples submerged in water. One of those samples would be 0° fiber orientation and the second would be 90° fiber orientation. The 90° sample which has mostly Direction A dominant diffusion, absorbed more than half than that with Direction B dominant diffusion (0°).

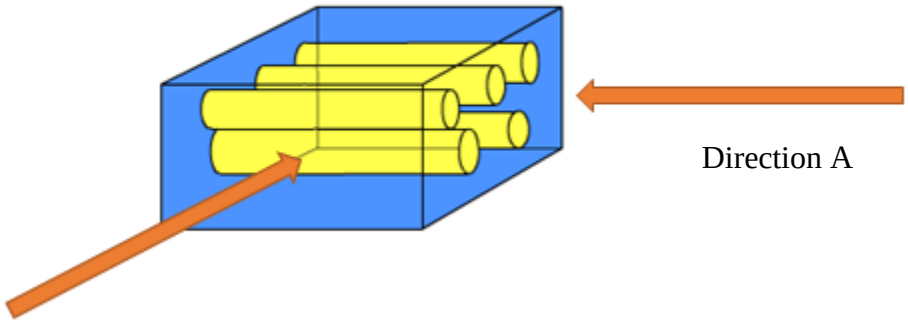

Figure 25. *Diffusional path experienced in unidirectional fiber composites. Direction A and B are considered as 0° and 90° fiber orientation respectively.* **(Brook, 2011)**

Degree of Crystallinity

Polymers can be amorphous or partially crystalline. Thermoplastic materials, are semi crystalline materials which depend on several factors such as cooling rate, thermal treatment, chain length, chain alignment, etc. (Askeland, 2014). Normally, polymer´s crystallinity varies between 30% up to 90 %, although 100% crystalline polymers are

hardly found. There is a tight relationship between the degree of crystallinity and mechanical properties in polymers (Chawla, 2012). Long chain structures in polymers play an important role when increasing ease of crystallization. The smaller the chain is, the less likely will be entangled between crystalline regions. In addition, branched chain molecules decrease the percentage of crystallinity a polymer can achieve. In Table 9, the degree of crystallinity of the three analyzed matrices is shown.

Table 9. *Degree of crystallinity (%) obtained from unprocessed PETG, PA 6/6, and PPS prepregs by differential scanning calorimetry.*

Material	Degree of Crystallinity (%)
PETG	34.11
PA 6/6	39.81
PPS	53.43

Establish Compression Molding Process Optimization for One of the Selected Material Systems.

In order to determine the optimum processing conditions for the selected material, two main variables will be taken into consideration: processing pressure and processing temperature. The effect of these variables will determine the optimum processing parameters considering mechanical performance (flexural strength and modulus). Flexural strength and modulus was defined as the measurable response of the processing variables due to the loading at which a leaf spring would be under during its lifetime. The main objective is to find the parameters that yield highest mechanical properties.

Design of Experiments (DOE)

After performing differential scanning calorimetry (DSC) on glass fiber reinforced PPS, a melting range from 525°f to 570°F was found. Considering the data obtained, three different temperatures were considered for the optimization analysis: 535°F, 550°F and 565°F. In addition, three processing pressures were analyzed: 5 tons, 7 tons and 10 tons. In Table 10, a summary of the combination of the considered processing parameters for the design of experiments is shown.

Table 10. *Selected process parameters for the proposed design of experiments (DOE). Two factors (Processing pressure and temperature) and three levels (low, medium, high) were used.*

	Processing Temperature (°F)	**Processing Pressure (tons)**
A1	535	5
A2	535	7
A3	535	10
B1	550	5
B2	550	7
B3	550	10
C1	565	5
C2	565	7
C3	565	10

A design of experiments 3^k was developed to determine the effect of each variable had on both flexural strength and flexural modulus. The three levels considered were

processing pressure at 5, 7 and 10 tons, whereas for processing temperature, 535°F, 550°F and 565°F was tested.

Results

One 12” by 12” glass reinforced PPS plate was processed for each of the possible combinations of parameters. From each of those plates, five samples in 0° fiber orientation and five samples in 90° fiber orientation were obtained. It is important to mention that each sample was selected from a different section of the plate to guarantee the uniformity of the results of the processing parameters on the plate.

In Figure 26, flexural strength and flexural modulus respectively in 0° fiber orientation are shown for each of the considered processing parameters. It can be recognized that, at higher temperature, higher flexural strength and modulus can be observed.

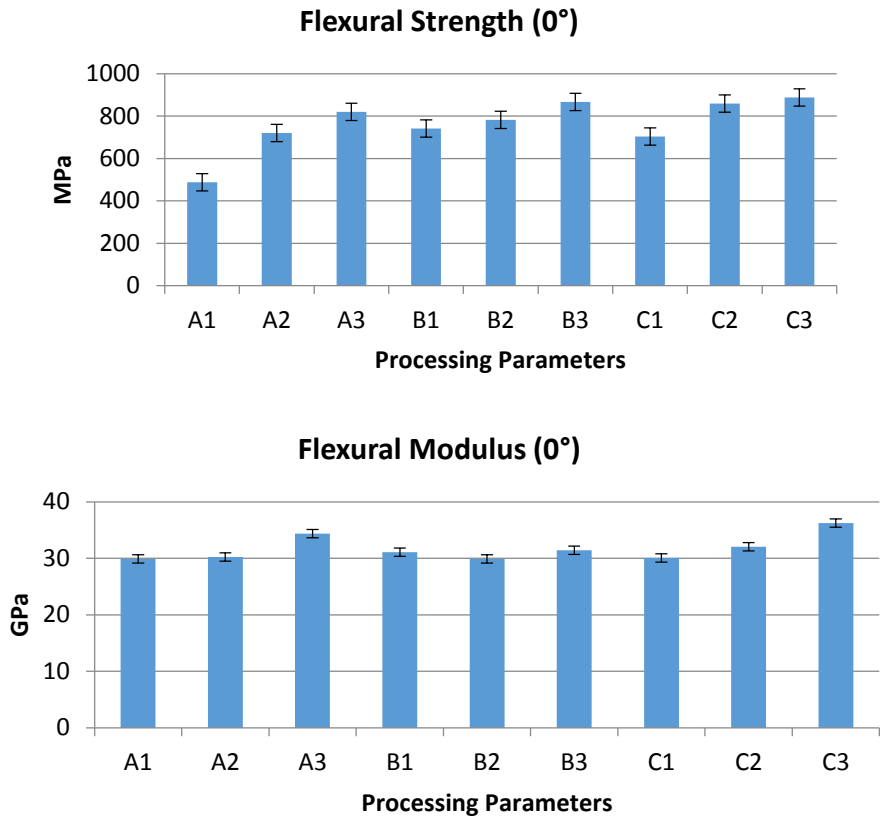

Figure 26. *Flexural modulus and strength at 0° fiber orientation for each of the considered processing parameters for unidirectional glass fiber reinforced PPS.*

In order to determine the effect of the two analyzed process parameters, MINITAB was used. In this software, the results of the flexural modulus for the 0° fiber orientation samples was analyzed. In Figure 27, the visual representation of the effect of these parameters as well as the interaction between them is shown. It can be identified that processing pressure has a direct effect on the modulus for glass fiber reinforced PPS composites.

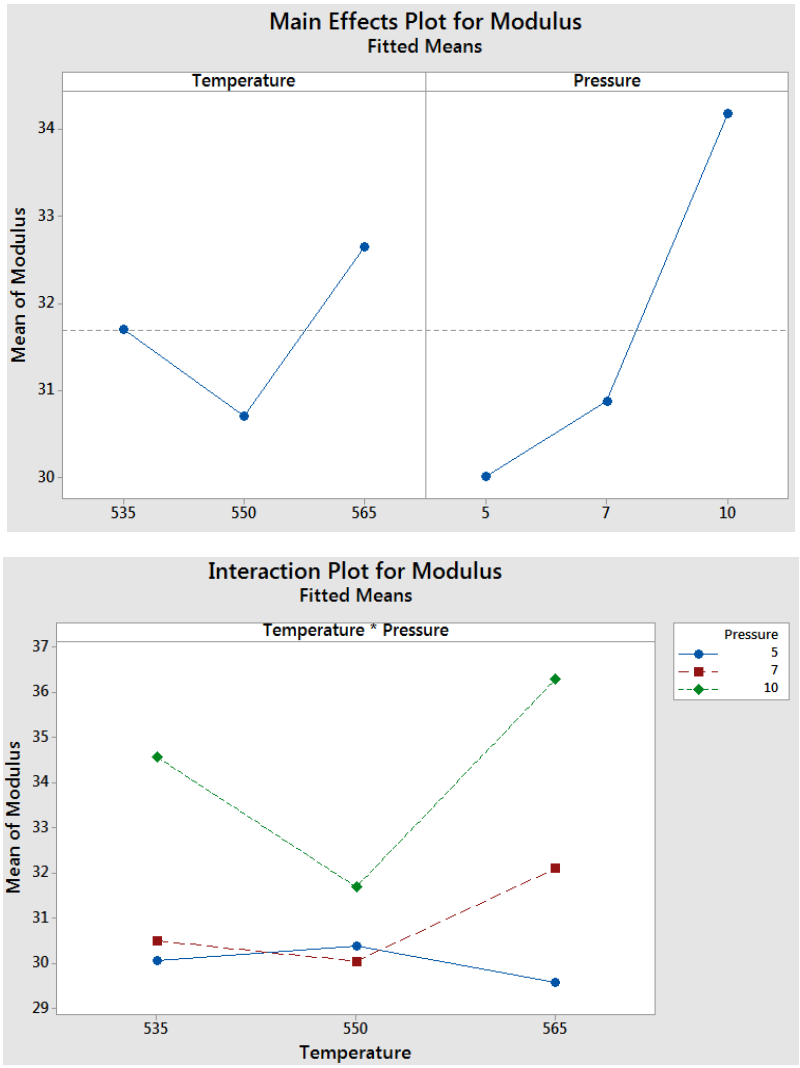

Figure 27*. Effect of processing temperature and processing pressure on flexural modulus for 0° glass reinforced PPS composites and the interaction between them.*

In Figure 28, flexural strength and flexural modulus respectively in 90° fiber orientation are shown for each of the considered processing parameters. As it was shown in 0°fiber orientation samples, temperature is yielding the higher flexural strength and modulus for the three considered processing pressures.

Similar to 0° fiber orientation samples, the effect of the two analyzed process parameters was made using MINITAB. The results of the flexural modulus for the 90° fiber

orientation samples were analyzed. In Figure 29, a visual representation of the effect of these parameters as well as the interaction between them is shown. It can be seen that processing pressure as well as process temperature have a direct effect on the flexural modulus for glass fiber reinforced PPS composites. Higher processing temperature and pressure yield the higher flexural properties.

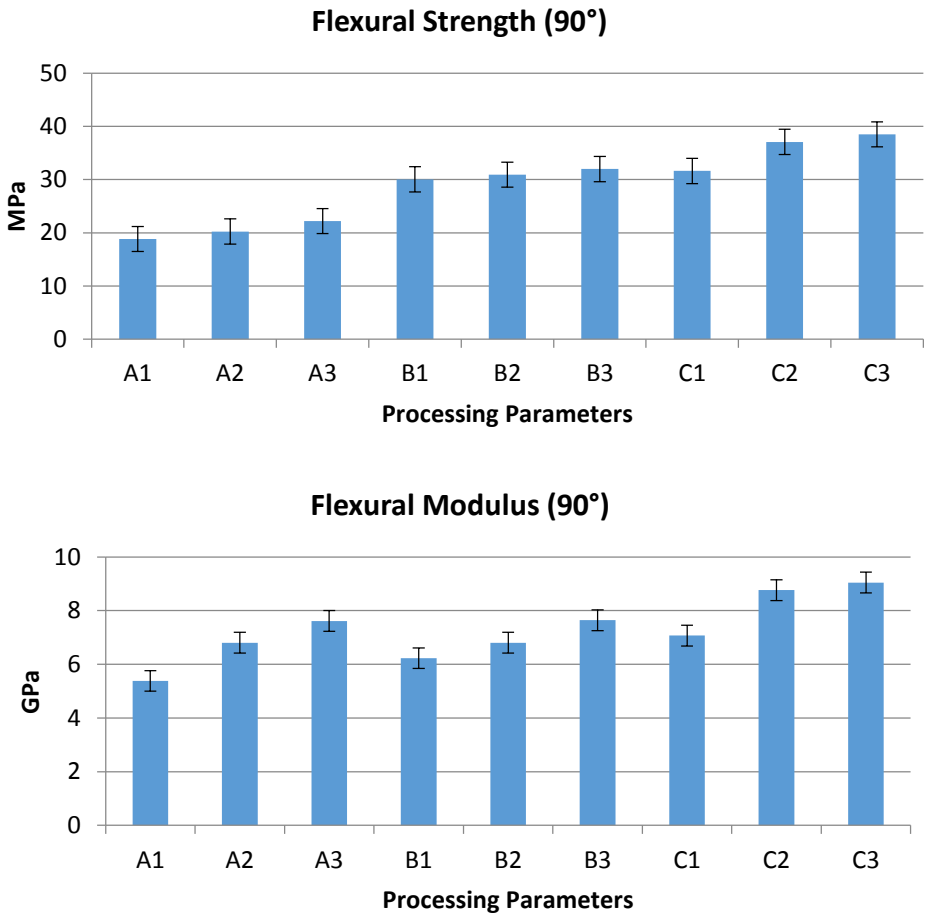

Figure 28. *Flexural modulus and strength at 90° fiber orientation for each of the considered processing parameters for unidirectional glass fiber reinforced PPS.*

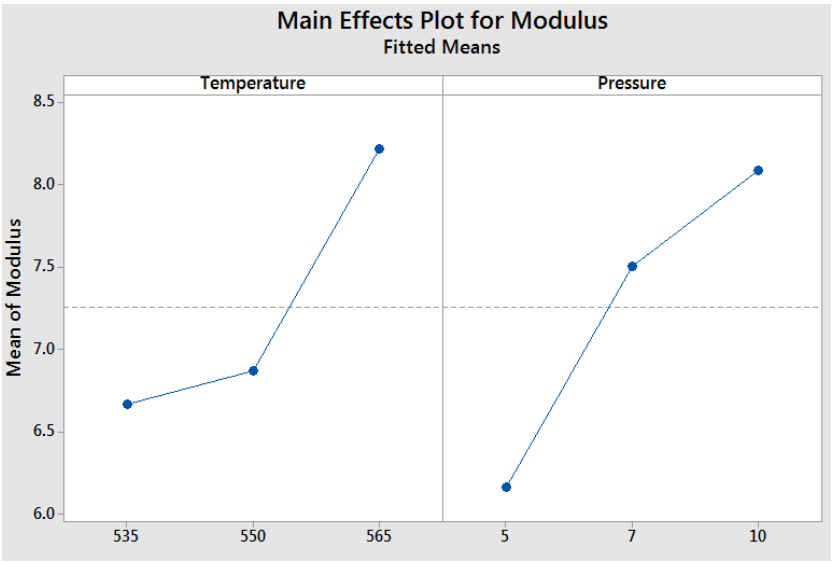

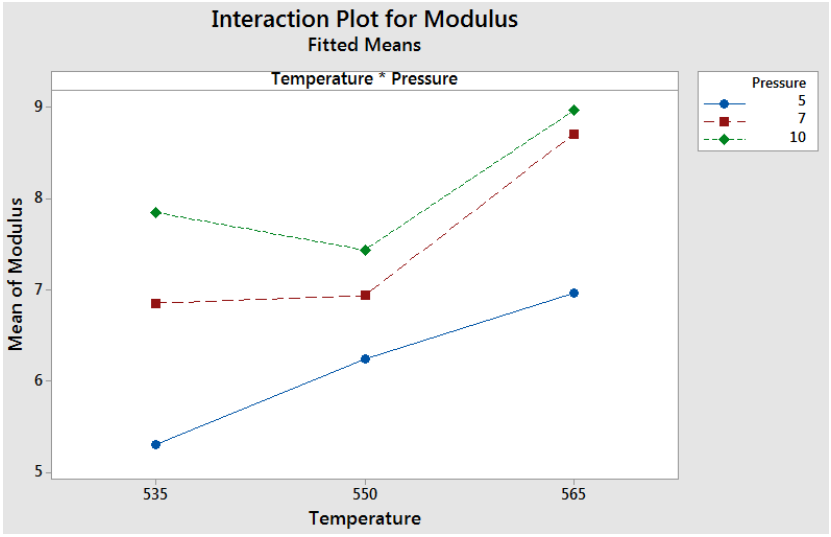

Figure 29*. Effect of processing temperature and processing pressure on flexural modulus for 90° glass reinforced PPS composites and the interaction between them.*

Degree of Crystallinity for Optimized Process

After analyzing the mechanical properties results for each of the defined processing parameters, DSC analysis was performed to determine the effect of the processing

parameter on the crystallinity of the polymer matrix. Recall that the degree of crystallinity in polymers is highly correlated with mechanical properties.

According to the flexural testing previously performed, the parameters that have the greatest influence in the mechanical properties of the PPS composite are high temperature and high pressure. In Table 11, the effect of pressure and temperature on the degree of crystallinity of glass fiber reinforced PPS is shown.

Table 11. *The effect of processing pressure (a) and processing temperature (b) on the crystallinity of glass fiber reinforced PPS.*

Sample	Crystallinity (%)	
535°F	43.19	10 tons
550°F	52.43	
565°F	56.39	

a)

Sample	Crystallinity (%)	
5 tons	63.40	565°F
7 tons	59.44	
10 tons	56.39	

b)

It can be identified that high processing pressure has an inverse effect on the degree of crystallinity, reducing it as pressure increases; whereas, when processing temperature is increased in result, the degree of crystallinity also increased.

Even though the degree of crystallinity is strongly related with the mechanical properties of a polymer; in this case, analyzed material being a composite, processing at lower pressure is not creating an optimum bonding between prepreg layers which translates in poor mechanical performance in the composite. According to Jun et.al, PPS shows this behavior when subjected to higher processing pressures. Polymer chains could be

constrained which limits the amount of ordered chain sections. This directly translates into lower crystallinity degree (Jun, 2007).

Correlate FEA Analysis with Experiments for Different Fiber Orientation Leaf Spring Lay Up

A glass fiber reinforced PA 6/6 helper spring was processed according to the parameters set for PA 6/6 sample processing. The prepreg layup sequence was determined after analyzing the thickness profile of an actual spring prototype provided by Rassini Suspensiones. This layup was designed to meet the dimensional requirements defined by Rassini Suspensiones by alternating different ply lengths according to the number of plies required per section. Each ply was considered 0.2003 mm in thickness after compression. Figure 30 shows the template in which the simulation of plies was developed.

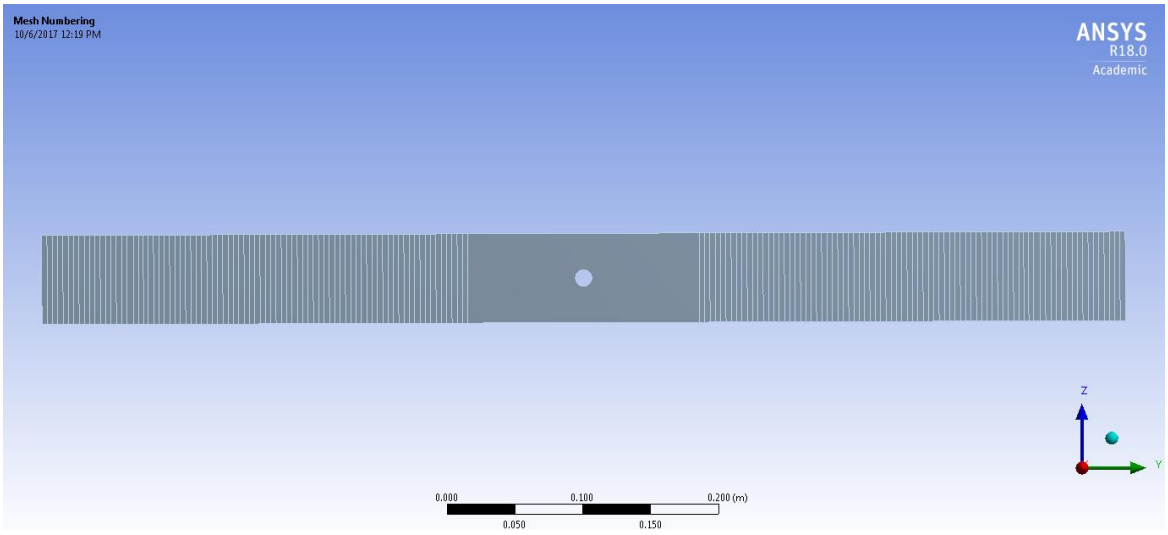

Figure 30. *Template utilized to define individual layer length of the tapered section of the helper spring.*

Two different fiber arrangements were considered for this analysis: Mid-Section Arrangement and Top and Bottom Arrangement. The prepreg layup was divided into three main zones: top, tapered and bottom section. The top and bottom section were considered as the section in which the plies had the length of the spring; whereas, the tapered section was the section located in the center of the spring in which layers were cut in different lengths to provide the taper required by Rassini Suspensiones. Five different sets of fiber angles were considered for this analysis: 0°, 15°/-15°, 30°/-30°, 45°/-45° and 90°. It is important to notice that the layup of the fibers considers stacking up the plies in an alternating fashion. In Table 12, a summary of the considered fiber arrangements is shown.

Table 12. *Considered fiber arrangements for FEA simulation. Mid –section arrangement and Top and bottom arrangement are divided into three main sections (top section, tapered section and bottom section).*

Fiber Arrangement	**Top Section**	**Tapered Section**	**Bottom Section**
Tapered Arrangement	0° Unidirectional	(15°/-15°, 30°/-30°, 45°/-45° and 90°)	0° Unidirectional
Top and Bottom Arrangement	0° Unidirectional except last 10 layers (15°/-15°, 30°/-30°, 45°/-45° and 90°)	0° Unidirectional	0° Unidirectional except last 10 layers (15°/-15°, 30°/-30°, 45°/-45° and 90°)

Simulation Parameters

The processed spring was four point flexural tested at Rassini Suspensiones facilities in order to determine the deflection rate (N/mm) and stress at specific deflection values.

Such testing was carried out following internal standard procedures which is summarized in Table 13. Figure 31 shows the set up utilized by Rassini Suspensiones for flexural testing is shown.

Table 13. *Four point bending set up conducted by Rassini Suspensiones.*

Supporting span	736 mm
Supporting pins	20 mm Ø
Loading pins distance	104 mm
First rate check	11.1 mm
Last rate check	33.3 mm
Max deflection	35 mm
Deflection increment	5 mm

Figure 31. *Four point testing setup utilized by Rassini Suspensiones.*

In Table 14, a summary of the considered mesh conditions for such model is displayed; whereas, in Figure 32, a visual representation of the distribution of the mesh in the helper spring FEA model is shown.

Table 14. *Mesh designing parameters for helper spring FEA simulation.*

Physics Preference	Mechanical
Mesh Size	$5x10^{-4}$m
Smoothing	Medium
Nodes	1688
Elements	1494
Edge Length	$3.6089x10^{-3}$
Rigid Body Behavior	Dimensionally reduced

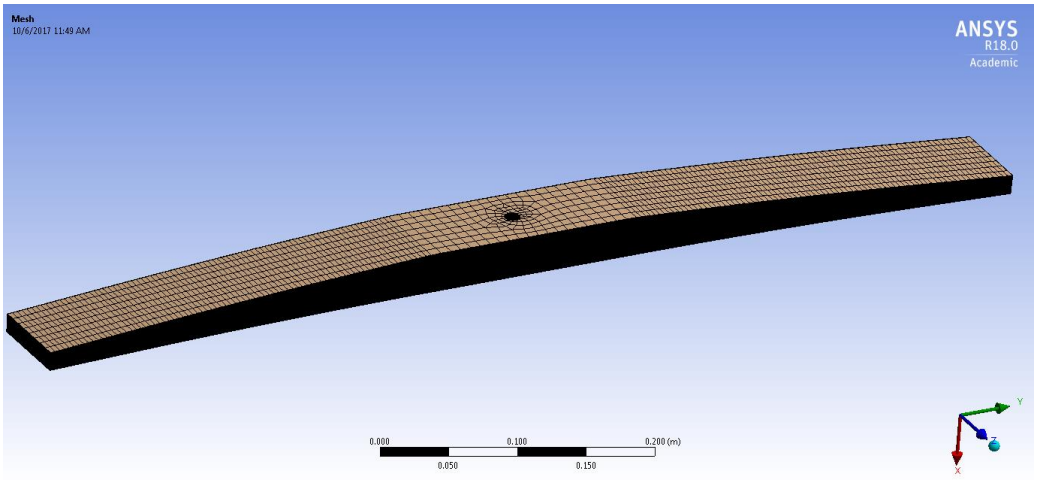

Figure 32. *Mesh distribution in FEA helper spring model.*

During its lifetime a leaf spring will encounter multiple types of loading such as vertical, lateral, torsional, etc. This simulation was aimed to find a fiber architecture that could

counter two main loading types: vertical and lateral. The main loading that a leaf spring will face is vertical; having said that, the optimum architecture should increase the lateral load capacity without sacrificing strength in vertical deflection. The location of the force and fixed elements for the lateral load and vertical load analysis is shown in Figure 33.

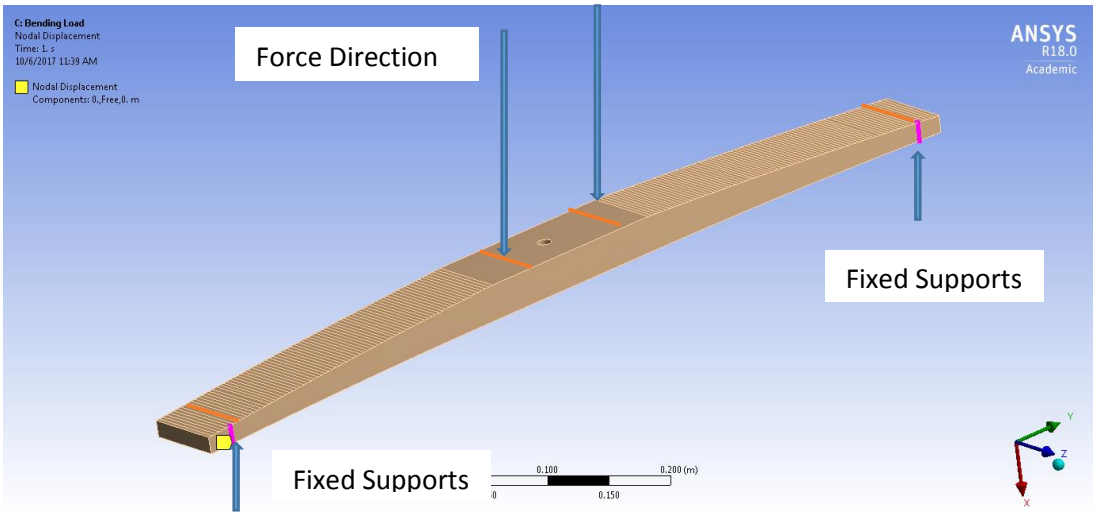

a)

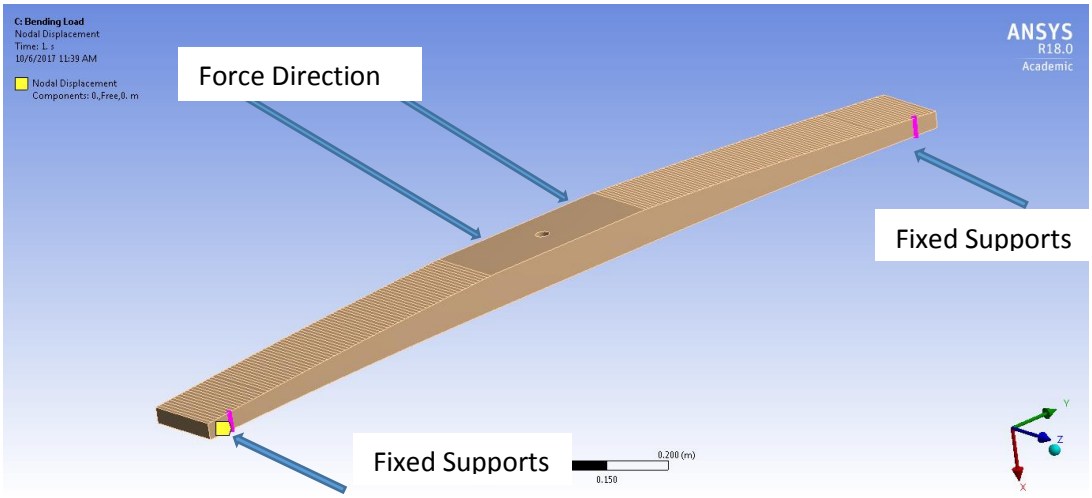

b)

Figure 33. *Force and supports setup for both a) Vertical load and b) Lateral load.*

The fixed elements for lateral loading were defined at 32 mm for the edge of the helper spring; whereas, the force lines were placed at 52 mm from the center hole of the spring.

These dimensions were stablished by Rassini Suspensiones according to internal design parameters and fixtures. FEA simulation final set up for both lateral and vertical loading is shown in Figure 34.

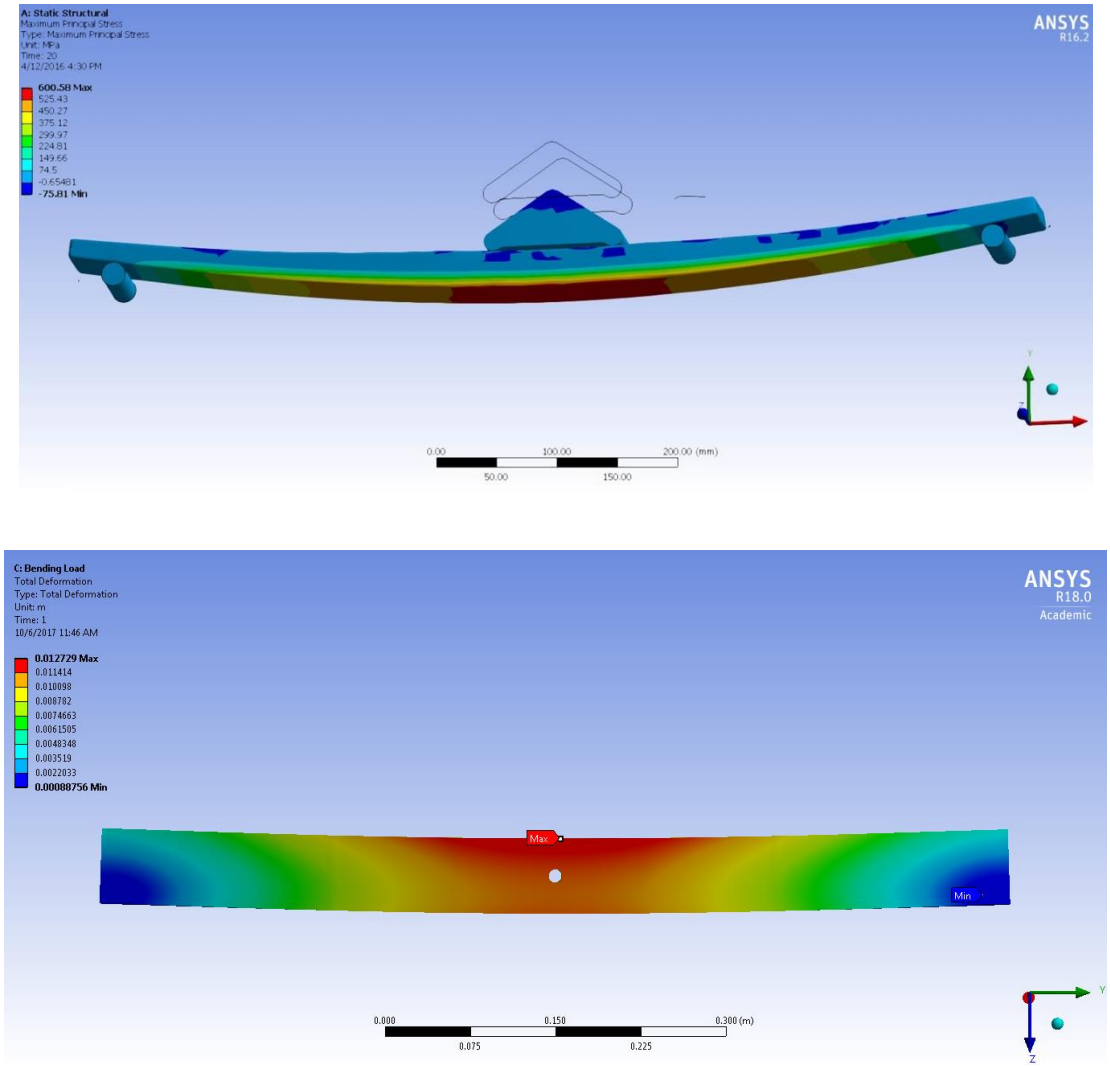

Figure 34. *FEA simulation final set up for both lateral (bottom) and vertical (top) loading*

FEA and Experimental Correlation

After recreating the processing and testing conditions in ANSYS, a comparison between experimental data and Finite Element Analysis (FEA) was made. In Table 15, a summary of the results for both experimental and FEA is shown. It is important to mention that the deflection rate was calculated as follows:

$$Deflection\ Rate = \left(\frac{(Load\ @\ First\ Rate\ Check - Load\ @\ Last\ Rate\ Check)}{Deflection\ @\ First\ Rate\ Check - Deflection\ @\ Last\ Rate\ Check}\right)$$

The loading utilized for the FEA model was the load used in the four point flexural testing at each deflection step. Strain gauges were placed at 5 mm from the center hole of the spring in both parallel and perpendicular to fiber orientation.

Table 15. *After simulating the actual testing conditions of the PA 6/6 helper spring, a comparison between experimental and FEA stress and deflection was made.*

	Experimental		FEA	
Load (N)	**Deflection (mm)**	**Stress (MPa)**	**Deflection (mm)**	**Stress (MPa)**
0	0	0	0	0
3071	5	61.72	5.12	57.66
6187	10	123.96	10.32	116.17
6908	**11.1**	**135.52**	**11.53**	**129.71**
9338	15	186	15.58	175.33
12329	20	247.76	20.58	231.48
15374	25	309.72	25.67	288.66
18240	30	371.88	30.45	342.47
20163	**33.3**	**414.64**	**33.66**	**378.57**
Rate (N/mm)	**597.08**		**598.96**	

When comparing the results of the deflection rate of both experimental and FEA, it could be proved that a correlation exists. An increment of 0.31% was shown in the FEA model when comparing deflection rate; whereas, when comparing stress, a decrement of 8.69% was shown in the FEA model. In Figure 35 and Figure 36, a visual comparison between FEA model and experimental values in terms of stress and deflection is made.

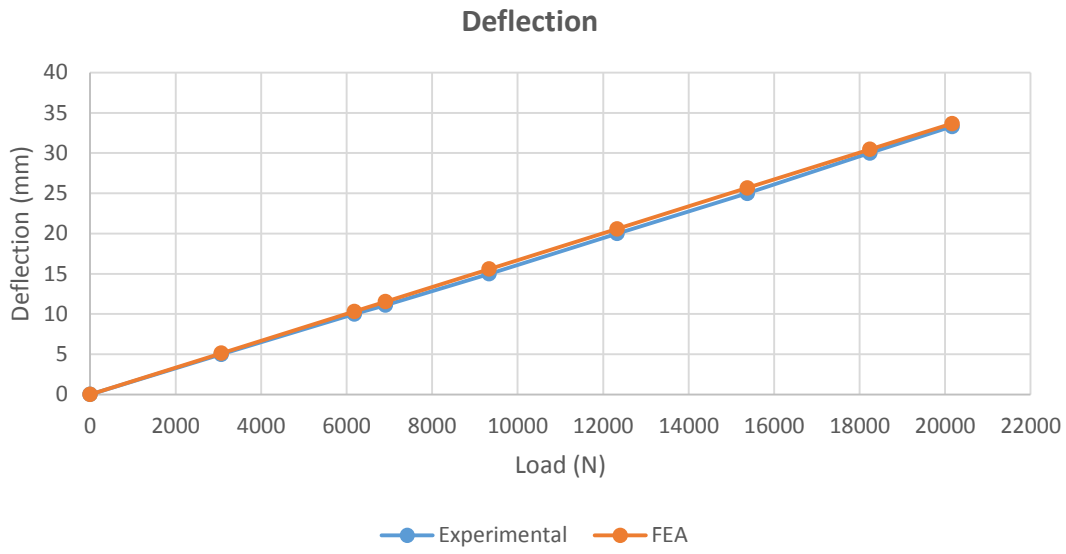

Table 35. *Deflection comparison between FEA modeling and experimental.*

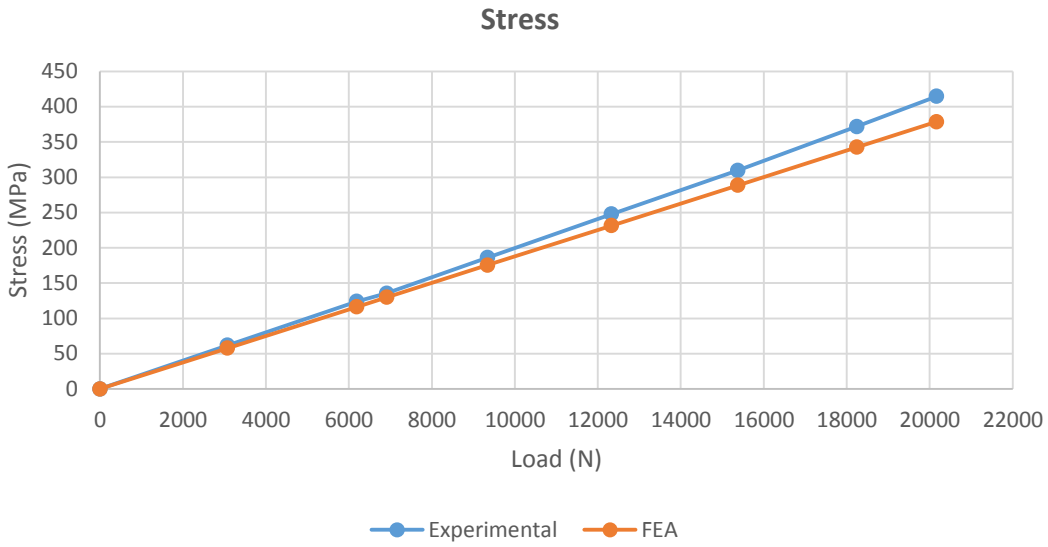

Table 36. *Stress comparison between FEA modeling and experimental.*

Fiber Arrangement Modification

Shifting the angle of the orientation of the fiber may decrease the strength of the composite in one direction but strengthen in another (W. J. Yu, 1988). Five fiber orientations were considered for this investigation: 0°, 15°, 30°, 45° and 90°. In Figure 37, the effect of fiber orientation on the helper spring when subjected to a vertical load for the tapered arrangement is shown.

In both fiber architectures, the best performance was achieved by the +/- 15° orientation. Vertical deflection increased 6 %, but stress was reduced by 5 %.

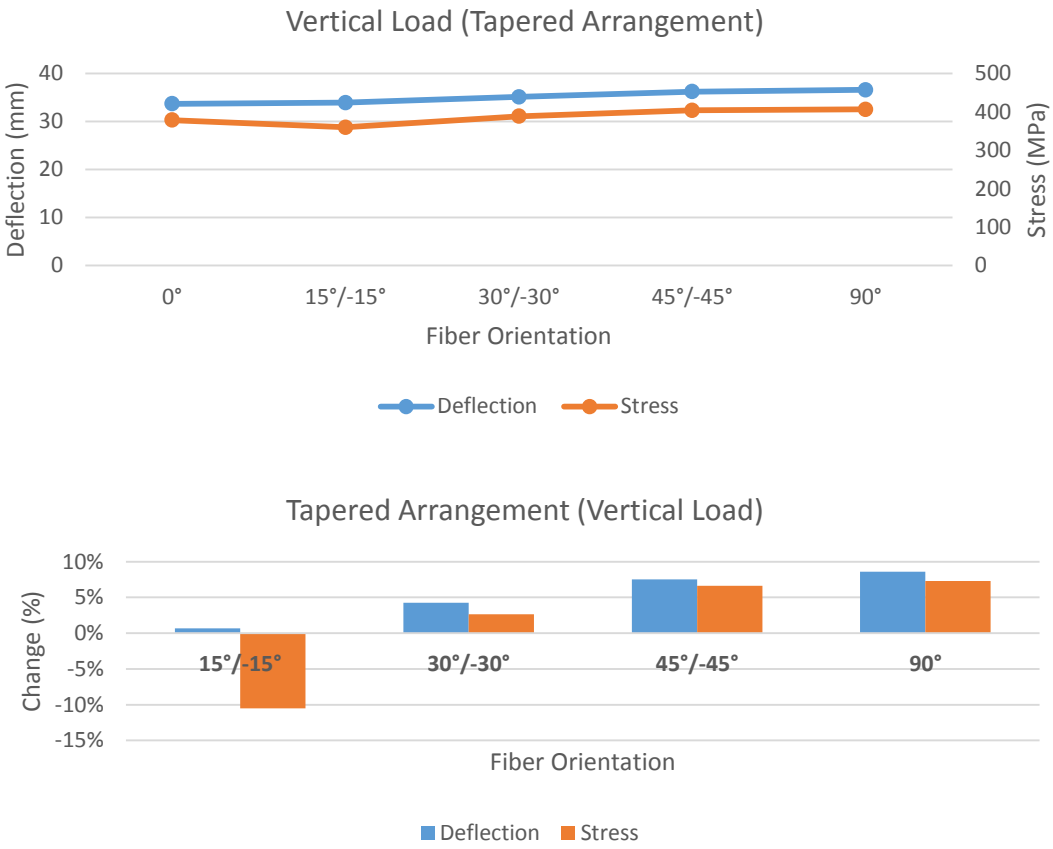

Figure 37. *Plotting of the effect of vertical loading on stress and deflection for the tapered arrangement.*

In Figure 38, the effect of fiber orientation on the helper spring when subjected to a vertical load for the top and bottom arrangement is shown.

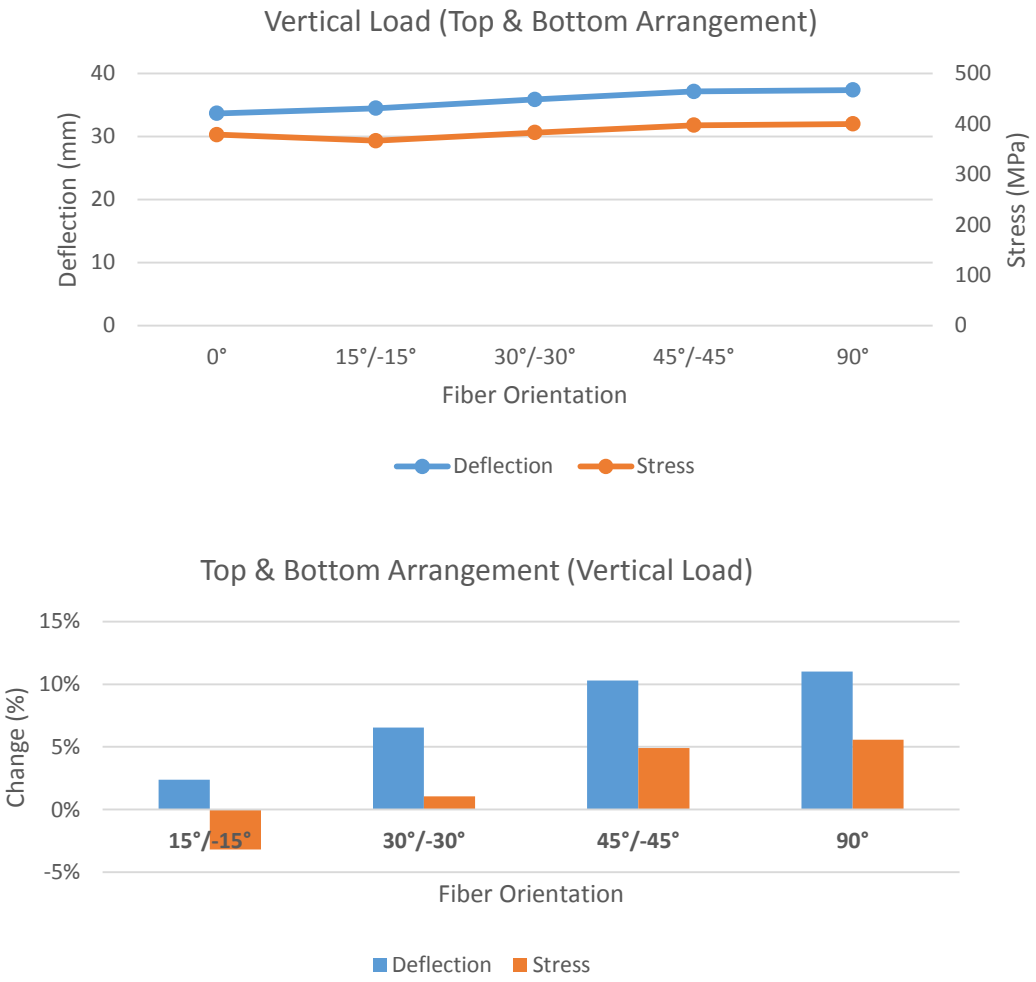

Figure 38. *Plotting of the effect of vertical loading on stress and deflection for the top and bottom arrangement.*

In Figure 39 and Figure 40, the effect of fiber orientation on the helper spring when subjected to lateral loading for both fiber architectures is shown. In both fiber architectures, the best performance was achieved by the +/- 15° orientation. Lateral deflection indicated nearly no change using this arrangement, but stress was reduced by 16%.

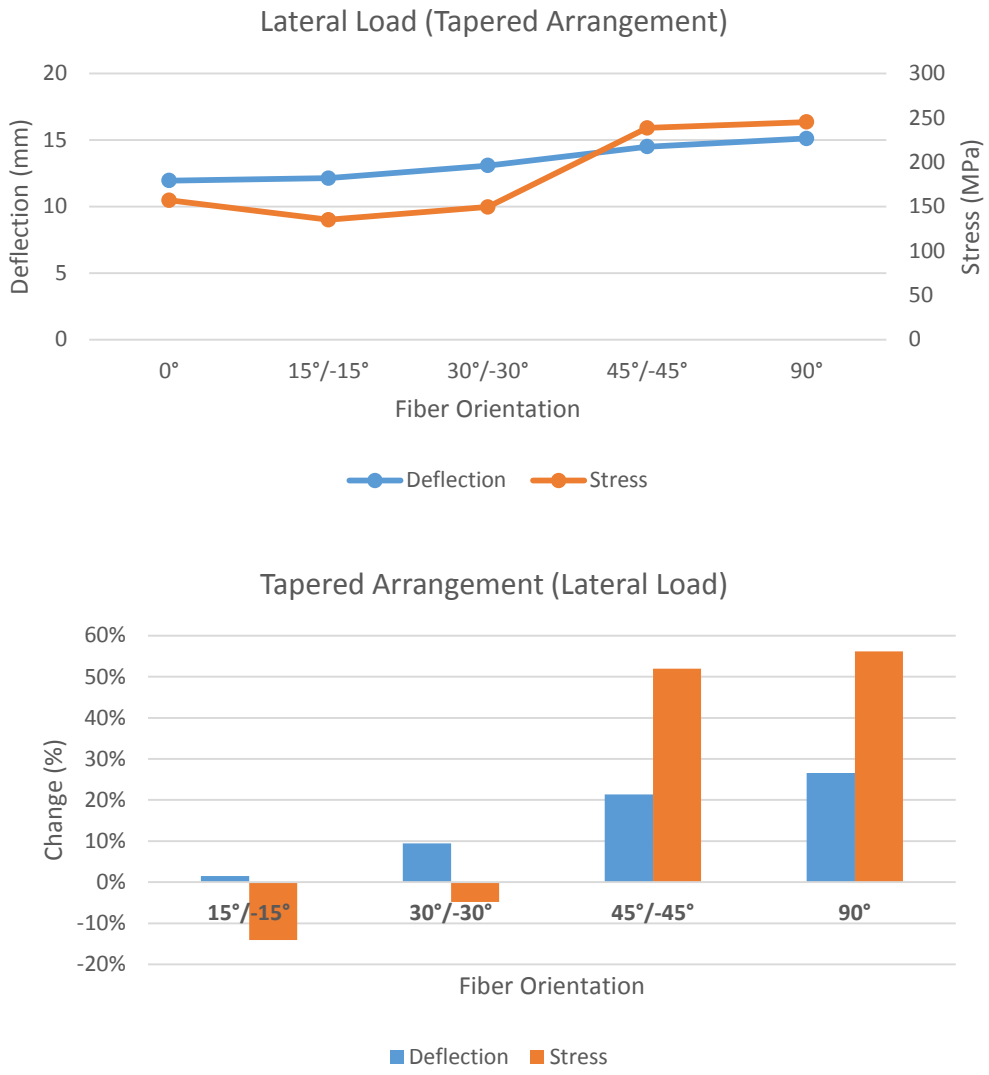

Figure 39. *Plotting of the effect of lateral loading on stress and deflection for the tapered arrangement.*

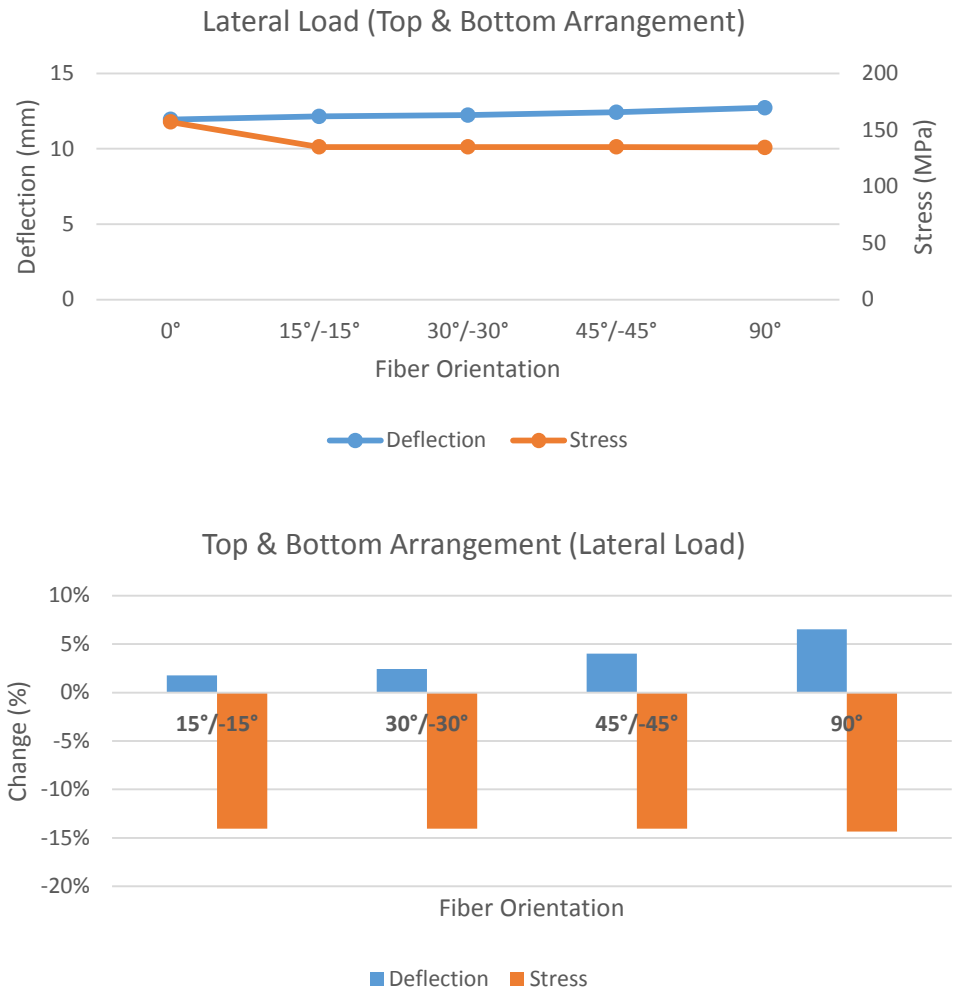

Figure 40. *Plotting of the effect of lateral loading on stress and deflection for the top and bottom arrangement.*

4. CONCLUSIONS

Three different glass fiber reinforced thermoplastic composites were compared to determine which yielded the properties that could replace steel for leaf spring applications. In order to accomplish this objective once a material was selected, processing optimization was conducted to obtain the best mechanical properties. FEA simulation was performed to modify the fiber architecture by rearranging the prepreg layup. The following conclusions could be drawn from the testing.

1. After analyzing three glass fiber reinforced composites (PETG, PA 6/6, PPS) the material that presented the best mechanical and moisture absorption properties suitable for leaf spring application is PPS. Although PETG retained its mechanical properties in a greater measure than PPS, dimensional changes and lower mechanical properties in non-exposed samples made PPS a best candidate to replace steel for leaf spring application.
2. A design of experiments was conducted to define the effect of processing pressure and processing temperature on the flexural modulus for glass reinforced PPS composites process by compression molding. Samples with 0° and 90° fiber orientation were analyzed. Both types of samples showed that processing pressure has a direct effect on the flexural modulus of the sample: at higher processing pressure, higher flexural modulus. However, processing temperature only showed this linear behavior for 90° fiber orientation samples. The higher flexural

properties are achieved with the configuration of 565°F (high temperature) and 10 tons (high pressure) for both 0° and 90° samples.

3. Once FEA simulation was conducted, it could be determined that the arrangement showing higher mechanical performance when subjected to lateral and vertical loading is the top and bottom arrangement. For both arrangements four different fiber orientation angles (15°, 30°, 45° and 90°) were analyzed. The configuration that showed the best lateral load was the tapered section with an alternating ply angle of 15°. This configuration reduced significantly the stress of the spring when subjected to both lateral and vertical loading.

REFERENCES

Albano, C., Sciamanna, R., Gonzalez, R., Papa, J., & Navarro, O. (2001). Analysis of Nylon 66 Solidification Process. *European Polymer Journal*, 851-860.

Al-Quereshi. (2001). Automobile Leaf Spring From Composite Materials. *Journal of Materials Processing Technology*, 58-61.

Askeland, D. (2014). *The Science and Engineering of Materials* . Boston: Cenage.

ASTM. (2005). *D5379 Standard Test Method for Shear Properties of Composite Materials by the V Notched Beam Method* . West Conshohocken: American Society of Materials and Testing.

ASTM. (2009). *D6641 Standard Test Method for Compressive Properties of Polymer Matrix Composite Materials Using a Combined Loading Compression CLC Test Fixture* . West Conshohocken: American Society of Materials and Testing.

ASTM. (2011). *D 3039 Standard Test Method forTensile Properties of Polymer Matrix Composites Materials.* West Conshohocken: American Society of Testing of Material.

ASTM. (2011). *D790 Standard Test Methods for Flexural Properties of Unreinforced and Reinforced Plastics and Electrical Insulating Materials.* West Conshohocken: American Society for Testing and Materials.

ASTM. (2014). *D 5229 Standard Test Method for Moisture Absorption Properties and Equilibrium Conditioning of Polym Matrix Composite Materials.* West Conshohocken: American Society for Testing and Materials.

ASTM. (2014). *Standard Test Method for Moisture Absorption Properties and Equilibrium Conditioning of Polym Matrix Composite Materials.* West Conshohocken: American Society for Testing and Materials.

ASTM. (2015). *D 3171 Standard Test Methods for Consituent Content of Composite Materials.* West Conshohocken: American Society of Materials and Testing.

Auborg, P. F., Crall, C., Hadley, J., Kaverman, R. D., & Miller, D. M. (1991). Glass Fibers, Ceramics. *ASM International*, 1027-1031.

Brook, D. (2011, February). *University of Cambridge*. Retrieved from https://www.doitpoms.ac.uk/tlplib/bones/index.php

Chawla, K. K. (2005). *Fibrous Materials.* Cambridge: Cambridge University Press.

Chawla, K. K. (2012). *Composite Materials.* New York: Springer.

Deaning, R. (1972). *Polymer Structure, Properties and Applications.* York: Cahners Publishing Company.

Deshmukh, B. B., & Jaju, S. B. (2011). Design and Analysis of Glass Fiber Reinforced Polymer (GFRP) Leaf Spring. *Fourth International Conference on Emerging Trends in Engineering & Technology.* Nagpur: IEEE.

Gaikwad, D., Sonkusare, R., & Wagh, S. (2012). Composite Leaf Spring for Light Weight Vehicle- Materials, Manufacturing, Process, Advantages & Disadvantages. *Int J Engg Techsci*, 410-413.

Gauthier, C., Chauchard, J., Chabert, B., Trotignon, J. P., Battegay, G., & Lamblin, V. (1993). Crystallization and Mechanical Properties of a Thermoplastic PET Reinforced with Unidirectional Glass Fiber. *Plastic, Rubber and Composites Processing and Applications*, 77-82.

Geiger, O., Henning, F., & Eyerer, P. (2006). LFT-D: Materials Tailored for New Applications. *Reinforced Plastics*, 30-35.

Grauer, D., Hangs, B., Martsman, A., & Tage, S. (2012). Improving Mechanical Performance of Automotive Underbody Shield with Unidirectional Tapes in Compression Molded Direct Long Fiber Thermoplastics. *Society for the Advancement of Material and Process Engineering*.

Harper, C. (2004). *Handbook of Plastics, Elastomers and Composites.* Lowell: McGraw-Hill.

Henshaw, J., & Weijian, H. (1996). An Overview of Recycling Issues for Composite Materials. *Journal of Thermoplastic Composite Materials*, 4-17.

IPCC. (2014). *Climate Change 2014 Synthesis Report.* Geneva: Intergovernmental Panel on Climate Change.

Joliff, Y. (2012). Experimental, analytical and numerical study of water diffusion in unidirectional composite materials – Interphase impact. *Computational Materials Science*, 141-145.

Jones, W. K., & Leach, D. C. (1993). Cost Effective Thermoplastic Composites. *38th International SAMPE Symposium*, 10-13.

Jun, L. (2007). Melt Crystallization and Morphology of PPS under high pressure. *Macromolecular Journal*, 405-414.

Juska, T. (1993). Effect of Water Immersion on Fiber/Matrix Adhesion in Thermoplastic Composites. *Thermoplastic Composite Materials*, 256-273.

Kim J, W., & Lee D, G. (2007). Effect of Fiber Content and Fiber Orientation on the Tensile Strength in Glass Mat Reinforced Thermoplastic Sheet. *Key Engineering Materials*, 337-340.

Knox, M. (2008). *Continuous Fiber Reinforced Thermoplastic Composites in the Automotive Industry.* Huntersville: Saint-Gobain Vetrotex America,.

Lopez, A., Martin, M., Diaz, I., Rodriguez, O., & Romero, M. (2010). Recycling of Glass Fibers from Fiberglass Polyester Waste Composite for the Manufacture of Glass-Ceramic Materials. *Journal of Environmental Protection*, 740-747.

Lou, A. (1988). Environmental effects on glass fiber reinforced PPS stampable composites. *Journal of Materials Engineering*, 109-116.

Lucas, J. (1992). Delamination fracture: Effect of fiber orientation on fracture of a continuous fiber composite laminate. *Engineering Fracture Mechanics*, 543-561.

Mahajan, S., Swami, S. C., & Patil, P. (2015). Experimental and FEA Analysis of Composite Leaf Spring by Varying Thickness. *International Journal of Research in Engineering and Technology*.

Mallik, P. K. (2007). *Fiber Reinforced Composites.* Dearborn: CRC Press.

Mathenulla, M., Sreenivasa, B., & Jaithirtha, R. (2014). Analysis of Glass Epoxy Reinforced Monolithic Leaf Spring. *International Journal of Modern Engineering Research*, 1-4.

MIT. (2008). *On The Road in 2035.* Massachusetts: Laboratory for Energy and the Environment.

Nase, M., Langer, B., Schumacher, S., & Grellmann, W. (2008). Toughness Optimization of Glass-Fiber Reinforced PA6/PA66 Based Composites: Effect of Matrix Composition and Colorants. *Journal of Applied Polymer Science*.

NetComposites Ltd. (2017). *NetComposites*. Retrieved from http://netcomposites.com/guide-tools/guide/reinforcements/fibre-cost/

Pandey, A., & Patil, A. (2014). Study of Fiber Reinforced Polymer (FRP) Leaf Spring – A Review. *Integrated Journal of Engineering Research and Technology*, 34-38.

Papacz, W., Tertel, E., Frankovsky, P., & Kurylo, P. (2014). Analysis of the Fatigue Life of Composite Leaf Springs. *Applied Mechanics and Materials*, 346-351.

Patel, H., Patel, V., Vishwakarma, A., & Ram, B. (2016). Review Over a Leaf Spring for Automobile Suspension System. *International Journal Research*, 469-472.

PolyOne. (2017, April). *PolyOne Advanced Composites*. Retrieved from http://www.polystrand.com/products/PDFs/Polystrand_Selection_Guide.pdf

Post, L., & van Dreumel, W. H. (1985). *Continuous Fiber Reinforced Thermoplastics.* Amsterdam: Elsevier Science Publishers.

Rajendran, I., & Vijayarangan, S. (2002). Design, analysis, fabrication and testing of a composite leaf spring. *Journal of the Institution of Engineers. India. Mechanical Engineering Division*, 180-187.

SAE. (2013). *SAE Manual on Design and Application of Leaf Spring.* Warrendale: Society of Automotive Enginners.

Sancaktar, E., & Gratton, M. (1999). Design, analysis, and optimization of composite leaf springs for light vehicle applications. *Composite Structures*, 195-204.

Sanjay, M. R., Arphita, G. R., & Yogesha, B. (2015). Study on Mechanical Properties of Natural - Glass Fibre Reinforced Polymer Hybrid Composites: A Review. *Materials Today: Proceedings*, 2959-2967.

Shokrieh, M., & Rezaei, D. (2003). Analysis and optimization of a composite leaf spring. *Composite Structures*, 317-325.

Smith, P. (2016). *The Effect of Ethanol, Methanol, and Water on the Hydrolyc Degradation of PA.* College of William and Mary.

Soules, D. A., Hagenson, R. L., & Cheng, P. J. (1991). Environmental Performance of Glass Fiber Reinforced PPS Advanced Thermoplastic Composites. *36th International Sampe Symposium*, 15-18.

Stanley, D. L. (1950). Compression Molding Thermoplastics. *Modern Plastics*, 107-111.

Stavrov, D., & Bersee, H. E. (2005). Resistance Welding of Thermoplastic Composites-An Overview. *Composites*, 39-54.

Subramanian, C., & Senthilvelan, S. (2010). Effect of reinforced fiber length on the joint performance of thermoplastic leaf spring. *Materials and Design*, 3733-3741.

Thomas, G. (2013, April 16). *AZO Materials*. Retrieved from https://www.azom.com/article.aspx?ArticleID=8353

Valentin, D. (1987). The hygrothermal behaviour of glass fibre reinforced Pa66 composites: a study of the effect of water absorptionon their mechanical properties. *Journal of Material Science*, 46-56.

W. J. Yu, H. C. (1988). Double Tapered FRP Beam for Automotive Suspension Leaf Spring. *Composite Structures*, 279-300.